2020

Measuring Differential Forest Growth in the Sheepscot River Headwaters with Bitemporal Lidar

Soren Denlinger
Colby College

Measuring Differential Forest Growth in the Sheepscot River Headwaters with Bitemporal Lidar

Soren A. Denlinger
Environmental Studies Program
Colby College
Waterville, Maine

May 18, 2020

A thesis submitted to the faculty of the Environmental Studies Program in partial fulfillment of the graduation requirements for the Degree of Bachelor of Arts with honors in Environmental Studies

Justin Becknell, Advisor	Philip Nyhus, Reader	Manuel Gimond, Reader

ABSTRACT

In recent years, lidar has proven itself as a forestry tool capable of accurate, large-scale inventories. Lidar has even shown utility in multitemporal analysis and growth assessment, given high-resolution or small-scale point clouds. However, lidar's efficacy as a multitemporal tool with relatively low-resolution, large-scale datasets is comparatively unknown. In this study, I compared forest in Midcoast Maine bitemporally, with publicly available datasets from the years 2007 and 2012. Specifically, I compared differences in growth characteristics of riparian, wetland, and upland forests. Although the 2007 dataset (created for geomorphological research) and the 2012 dataset (statewide, general-purpose) possess varying point densities and differ in intended use, I detected meaningful change between the two years, though not between these three classes of forest.

Between 2007 and 2012, riparian, wetland, and upland forests grew roughly 140 centimeters. However, these gains were largely balanced out by a similar rate of harvest. In maps of canopy height difference between the two years, these disturbances are particularly visible. Specific forest management styles are also discernable, from clearcuts to thinning. The level of detail and forest growth visible in this study affirm lidar's value in multitemporal analysis, despite relatively low resolutions. As lidar point clouds grow in quality and quantity, so will their value to future research.

ACKNOWLEDGEMENTS

I am indebted to many in the Environmental Studies program for the completion of this thesis. First, I would like to thank Justin Becknell for advising me from this study's inception to completion. My work in his Colby Forest Ecosystems Lab in 2018 and 2019 introduced me to lidar as a forest research tool and laid the groundwork for my continued interest in its applications.

I also owe thanks to Manuel Gimond for his feedback and input towards this thesis. As a student in his Exploratory Data Analysis in R, I first appreciated the utility, power, and elegance of R. Thanks to his lessons in both R and ArcGIS, data analysis during the course of this study was much less painful than expected.

I am also indebted to Philip Nyhus for his academic advising and GIS instruction throughout my years at Colby. I can trace my continuing interest in cartography and geographic information systems back to his introductory GIS class during my sophomore year.

Finally, I would like to thank two strong formative influences on my passion for forest conservation. First, thanks to Judy Stone for her lessons in tree identification and physiology. Exploring forests and landscapes as a whole are more informative and enjoyable thanks to her. Second, I owe thanks to the staff of the Blue Hill Heritage Trust, where I worked during the summer of 2019. George Fields, Sandy Walczyk, Chrissy Allen, Landere Naisbitt, Hans Carlson, and Beth Dickens introduced me to a hands-on, community-based land trust and fueled a passion for inclusive, equitable conservation. I owe much of my familiarity with land conservation to them.

TABLE OF CONTENTS

INTRODUCTION

Lidar as a Forestry Tool

In the past twenty years, lidar has emerged as a powerful tool for the conservation and management of forests (Lim et al. 2003, Asner et al. 2012, Farrell et al. 2013). At a basic level, lidar operates by timing the return of laser pulses from an airplane, car, or other point source to measure distance from a target (Lim et al. 2003). When aimed at a forest from above, the pulses can bounce off of tree canopies, the ground, or any point in between. Thus, they offer a three-dimensional view of the forest in what is known as a 'point cloud'. Within this point cloud, lidar analysts can quantify canopy height, profile, and spatial forest variability (Dassot et al. 2011). Point clouds can also be used to estimate tree height, basal area, aboveground biomass, canopy closure, and stem density (Lim et al. 2014). This analysis can generate data valuable in the management of both forests and wildlife.

While much data can be derived from lidar point clouds, analysis has often been limited to a single snapshot of the forest. Performing change analysis with lidar datasets represents a nascent form of study, as a dearth of spatially overlapping multi-temporal datasets has prevented its wide-scale adoption. Various factors such as missing georectification, low point density and accuracy, and seasonal variability across datasets create uncertainty with regard to the feasibility of multitemporal comparisons, which I will describe in greater detail later on (Eitel et al. 2016). Despite these obstacles, this type of analysis retains immense potential due to lidar's unparalleled ability to efficiently survey large blocks of land (Lim et al. 2003). Even large-scale, low-density datasets have been used to derive forest-scale metrics in New England, although these measurements poorly estimate the characteristics of individual trees (Hayashi et al. 2014). Additionally, lidar offers the potential to compare different types of forests (e.g. riparian, upland, or wetlands) in the same region at nearly identical points in time.

Successful examples of change analysis in lidar are becoming more common. Multitemporal lidar analysis is easily used for comparison before and after catastrophic events. For instance, widespread snow damage, landslides, and forest fires are all potential subjects of study (Vastaranta et al. 2012, Ventura et al. 2011, Wulder et al. 2009). In boreal forests, stand-scale changes were observed as early as 2008, along with

lidar-based structural canopy analysis in 2010 (Vepakomma et al. 2008, Vepakomma et al. 2010). Ma et al. (2017) measured changes in tree growth in California's Sierra Nevada with airborne lidar and found them to be consistent with field measurements. In both tropical and subtropical forests, this capability has been exploited in the estimation of biomass dynamics (Englhart et al. 2013, Cao et al. 2016, Becknell et al. 2018). Even sub-annual growth was detectable in small-scale datasets in Scotland, given high-resolution point clouds (Zhao 2018). However, while differential species identification, mapping, and growth dynamics have been examined for riparian, upland, and wetland forest individually, direct comparison of the growth differences in these three forest types with bitemporal lidar is a relative unknown (Gilmore et al. 2008, Englhart et al. 2013, Michez et al. 2016).

Research Questions

This study is guided by several overarching questions. Is direct temporal comparison of forests possible between two disparately created lidar datasets? And if so, is it possible to measure growth differences in forest type (riparian, upland, and wetlands) over time in remotely sensed characteristics like forest height and structural complexity? What other patterns are visible from exploring this multi-temporal lidar dataset? By comparing these two datasets, I aim to both answer these questions and lay groundwork for future studies of different locations.

Application in Maine

Three forest types are particularly common to Maine: upland, wetland, and riparian (Gawler and Cutko 2018). Each type of forest is composed of different woody plants, hydrologies, and nutrient availability (Niswander and Mitsch 1995, McGlynn et al. 1999, Campbell et al. 2000, McKinney and Charpentier 2008, Ricker et al. 2013, Gawler and Cutko 2018). Riparian forest, by virtue of its location along streams and rivers, often contain nutrient-rich alluvial soils and more humid conditions than other locations (Bromley 1935, Chen et al. 1999, Brooks and Kyker-Snowman 2009). Wetland settings are often limited in nutrients and characterized by low rates of decomposition and plant growth (Gotelli 2008). Upland forest is more likely to possess xeric soils and otherwise dry conditions (Ohmann and Grigal 1985, Copenheaver et al. 2000). Therefore, it follows that forest growth rates could potentially vary across these three

forest settings (Toledo et al. 2010). Additionally, changes in forest structure could vary as well due to different species compositions and hydrological constraints (Laser et al. 2009). In comparing growth across these three forest types, these differences in forest attributes may be detectable across two lidar point clouds collected at least one growing season apart.

Though spatially overlapping, time-disparate datasets are uncommon in New England, the watershed of the Sheepscot River in midcoast Maine offers an opportunity for such analysis. A lidar dataset from the fall of 2007 covers 320 km^2 of the region, originally intended to probe the influence of land use, climate, and geology on alluvial processes (Snyder 2013). Its narrow focus corresponds with relatively high point densities and vertical accuracy, especially for a dataset of its age. A larger overlying dataset encompassing the same spatial extent was collected in the spring of 2012 for the Maine Office of GIS (known as MEGIS) for use in a variety of applications, from land use planning to risk management (OCM Partners 2019). As a result, the 2012 MEGIS dataset was flown at a higher altitude with wider flightlines than the 2007 dataset to gather data more quickly. These efficiencies came at the cost of data quality, leading to both less accuracy and fewer overall points. Despite these differences in accuracy and point density, these two datasets still offer the opportunity to bitemporally analyze the intersecting forest across four growing seasons.

Study Area

The spatial overlap of the datasets in the Sheepscot headwaters lies primarily in Kennebec and Waldo Counties, and specifically the towns of Windsor and Palermo (Figures 1, 2). Portions of China, Somerville, and Whitefield are also included (Figure 1). Approximately 20% of the land in the Sheepscot River watershed is agricultural, and forests compose between 75% and 95% of the remainder (McLean et al. 2007). These forests are largely deciduous, dominated by northern hardwoods like sugar maple (*Acer saccharum*), red maple (*Acer rubrum*), American beech (*Fagus grandifolia*), and northern red oak (*Quercus rubra*) (McWilliams et al. 2004). Spruce (*Picea sp.*) and eastern white pine (*Pinus strobus*) are also common. Most forests in the study area occupy former farmland, and thus represent second- or third-growth forest (McLean et al.

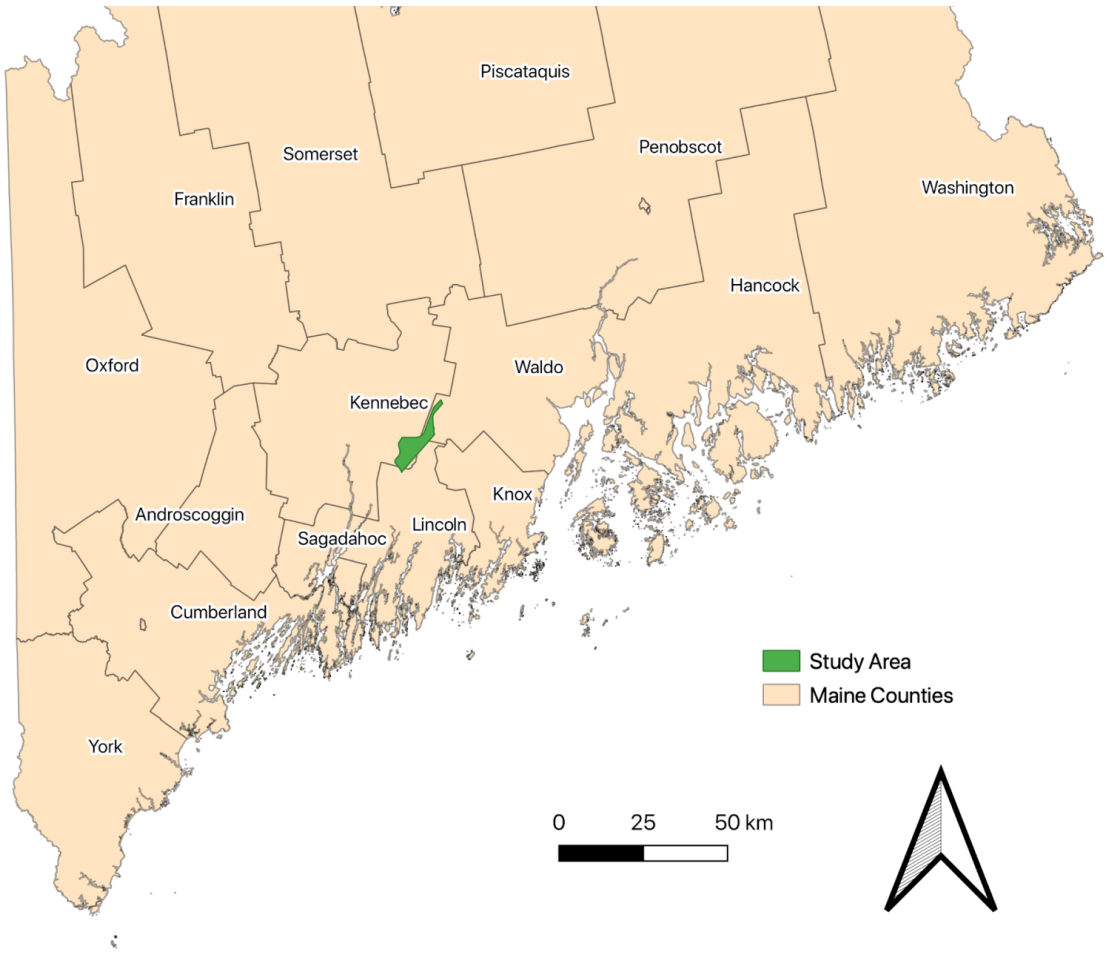

Figure 1. Study area in relation to southern Maine.

2007). According to estimates from the Maine Forest Service (2010), 1-2% of this forestland is harvested each year. In terms of hydrologic features, Beech, Savade, and Turner Ponds lie within the study area. Both the West and East Branches of the Sheepscot River drain the area, meeting near its southern end. The Sheepscot River is also home to one of the few remaining populations of wild Atlantic Salmon (Laser et al. 2009). Along the West Branch, stands of relatively small red maple and balsam fir compose the riparian forest (Laser et al. 2009). Though predominantly rural, the study area also includes some developed areas in the vicinity of Windsorville and Windsor Station.

METHODS

The Sheepscot River area's spatially intersecting datasets, rural nature, and variety of riparian, wetland, and upland forest combine to increase its value to this study.

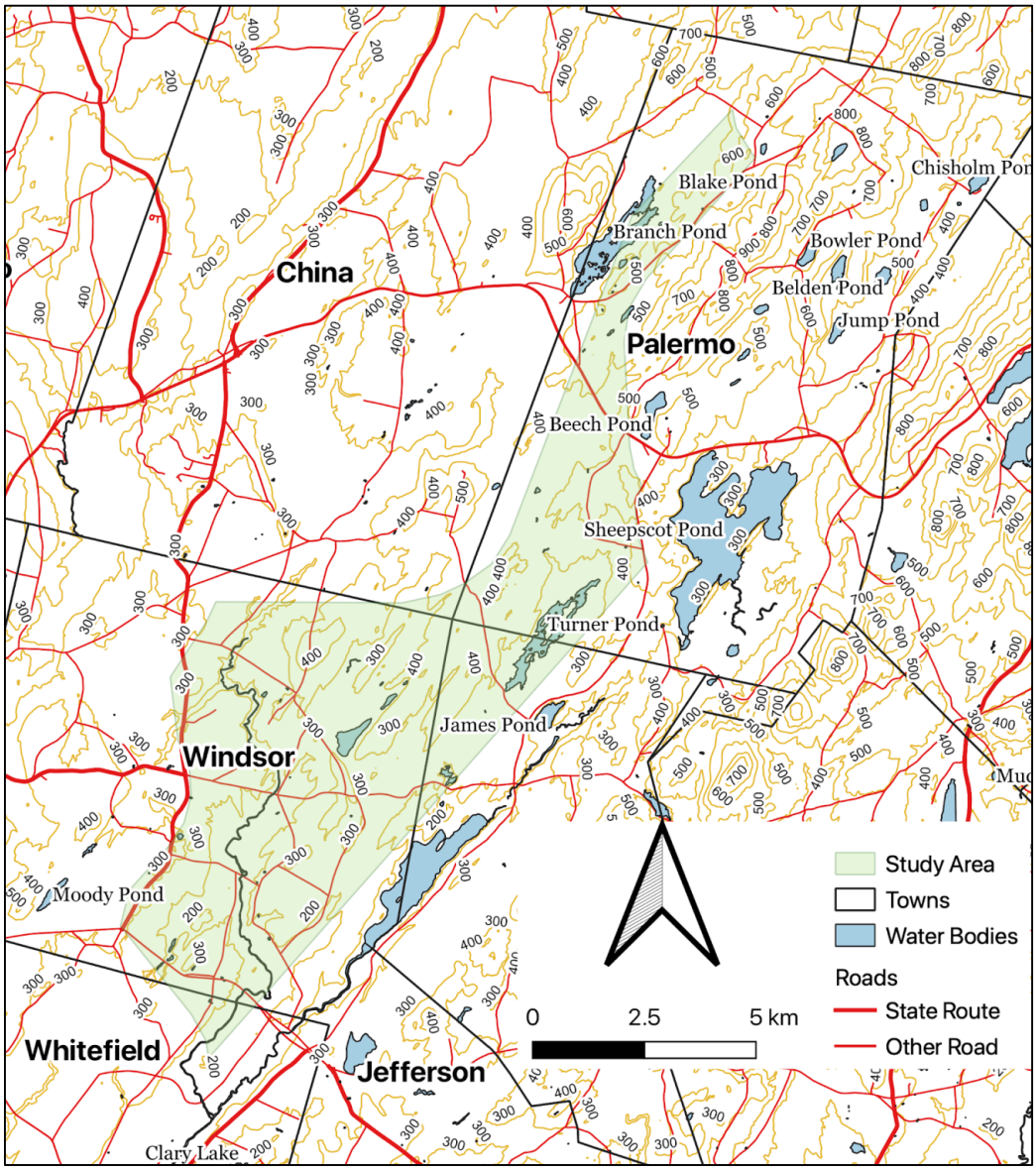

Figure 2. Study area in Midcoast Maine.

I trimmed this dataset to remove any potential edge effects by excluding 500 meters on the edges, and treated the resulting area as the study area. From here, I assessed any potential error within the study area and the datasets before moving on.

Error Assessment

Appropriate assessment of error is necessary in order to ensure the validity of comparisons between the 2007 and 2012 datasets. Because the two surveys utilized different airborne sensors (Optech Gemini in 2007 and both Leica ALS60 and Optech Gemini systems in 2012), it is possible that the two surveys recorded systematically

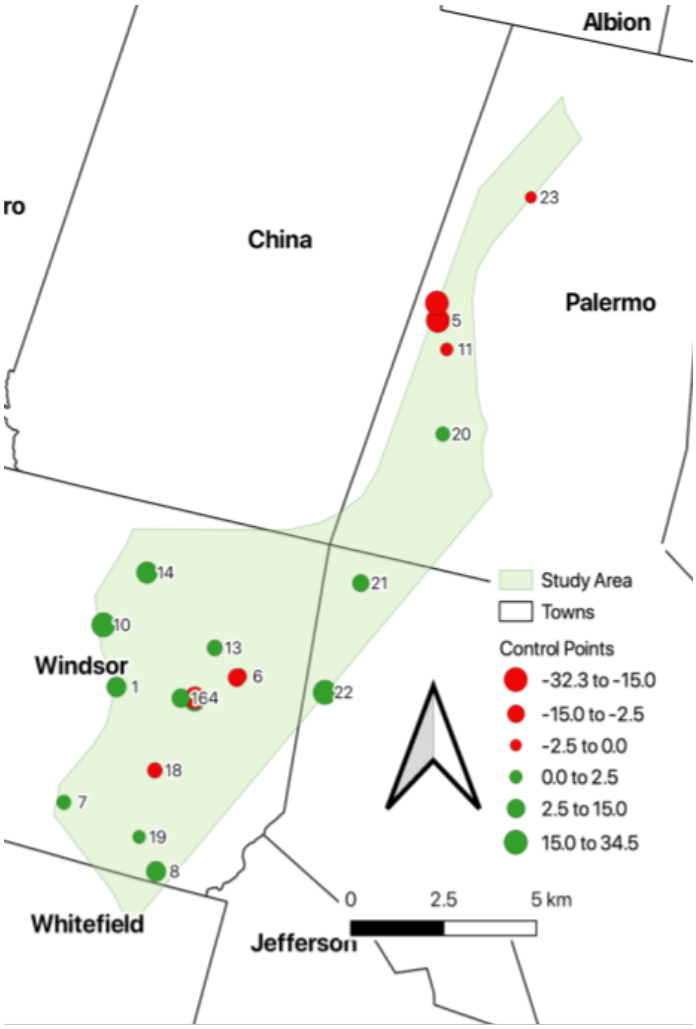

Figure 3. Control points, scaled and colored by difference between 2012 and 2007 peaks.

different measurements (Snyder 2013, OCM Partners 2019). Therefore, to ensure consistency between the two, static control points must vary within the two surveys' margins of error, as described by the datasets' authors. Specifically, given estimates of 12.5 centimeters of horizontal error in the 2007 dataset and 25.0 centimeters in 2012, measurements of control points like flat roofs and road surfaces must vary by less than the larger 25.0 centimeters to rule out error in one or more of the point clouds (Table 1). For angled surfaces that could include both components of both horizontal and vertical error, control points must fall within the value described by the expression $\sqrt{vertical^2 + horizontal^2}$ since this represents the hypotenuse.

Table 1. Stated margins of error for two datasets.

	2007	2012
Vertical	6.4 cm	12.5 cm
Horizontal	10.0 cm	25.0 cm
Total	11.9 cm	28.0 cm

To ensure this variation does not reflect systematic error across the two datasets, I surveyed a variety of fixed control points across the study area (Figure 3). These control points included road surfaces, roofs, and bridges. To assess the height differences between 2007 and 2012, I compared Z value peaks on point return density charts. More specifically, I subtracted the peak from the 2007 data from the 2012 peak to derive either a positive or negative number. I also performed a Moran's I spatial autocorrelation in R 3.6.3 using the spdep 1.1-3 and a search radius of five kilometers with Universal Transverse Mercator coordinates, Zone 19N. (Bivand et al. 2013, R Core Team 2019). These measures sought to validate the quality control performed on both surveys. In 2007, this consisted of two control points constrained to within two centimeters' accuracy through GNSS measurement and post-processing, as well as post-processing of the airplane's trajectory and measurements (Snyder 2013). The 2012 dataset similarly utilizes two on-the-ground control points and post-processing of airplane dynamics performed by Woolpert for the Maine Statewide Orthoimagery Program (OCM Partners 2019).

Assessment of the density and distribution of point returns is also necessary before unbiased comparisons can be made across the two datasets. Point densities are markedly different: 5 to 6 pts/m^2 in the 2007 dataset and 1.5 to 2 pts/m^2 in 2012. This is largely a product of the 2007 dataset's smaller spatial extent, despite its age. This means that extreme points, such as the tops of the tallest trees, are more likely to be captured in the 2007 dataset than in 2012. This has the potential to skew canopy height maps, though density curves should be relatively unaffected. Additionally, the distribution of point returns is similar between the two datasets. Flight lines were flown within 20º of each other (2007 at a bearing of 132º and 2012 at 115º), resulting in only minor differences between their alignment.

These measurable differences between static control points in each dataset are too small and randomly distributed to correct. Therefore, for the purposes of this study, I treated the two datasets as effectively precise. While differences remain in terms of seasonality and point density, I regarded each individual point as an accurate reflection of the conditions measured at the time of collection.

Lidar Data Processing

To compare growth differences across disparate forest types, I classified the study area into riparian, upland, and wetland forests (Figure 4). I used the National Wetland Inventory's classifications of wetlands to both save time and avoid classification bias and error. This dataset was also useful in excluding open water from ponds and lakes. I classified forests within 100 meters of streams and rivers as riparian forests, using the most conservative buffer width as outlined by Yale School of Forestry researchers. (Hawes and Smith, 2005). I used stream flowlines delineated by the National Hydrography Dataset as the basis for these buffers. The remainder of the study area was classified as upland forest. To remove farm fields, roads, powerlines, and developed areas from all three forest categories, I selected only land rated above 50% forest cover from the National Land Cover Dataset (NLCD). To remove land outside of this criteria, I created a new raster from the NLCD data containing only pixels with forest cover above 50%, and then clipped the forest types to fit this new raster. These steps resulted in three polygons covering the entirety of undeveloped riparian, upland, and wetland forest for the study area.

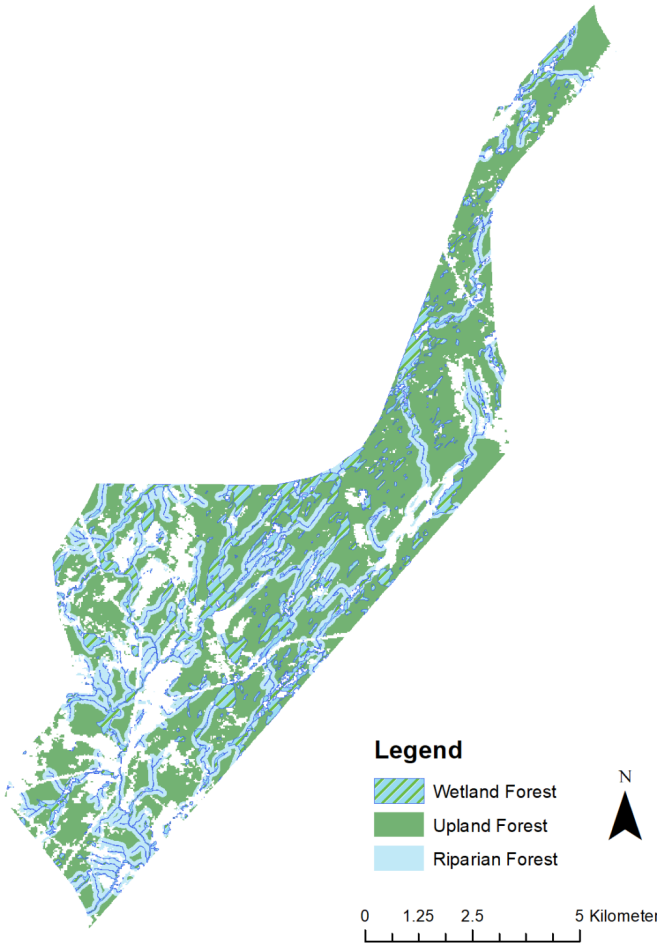

Figure 4. Assigned forest types within Sheepscot River headwaters.

I then processed the entirety of the intersected area for both 2007 and 2012 point cloud using R version 3.6.3 (2019), with most analysis making use of Jean-Romaine Roussel and David Auty's lidR package, version 2.2.0 (2020). Each year was downloaded in 8-12 tiles, small enough to be processed individually on desktop machines. After loading each year's data, I classified the point clouds into ground and non-ground points. I then used this classification scheme for normalization. Normalizing the point clouds removes the underlying topography, using a k-nearest neighbors approach (Figure 5). I then removed all ground points to reduce the computational load. For each year and forest category (riparian, upland, and wetlands),

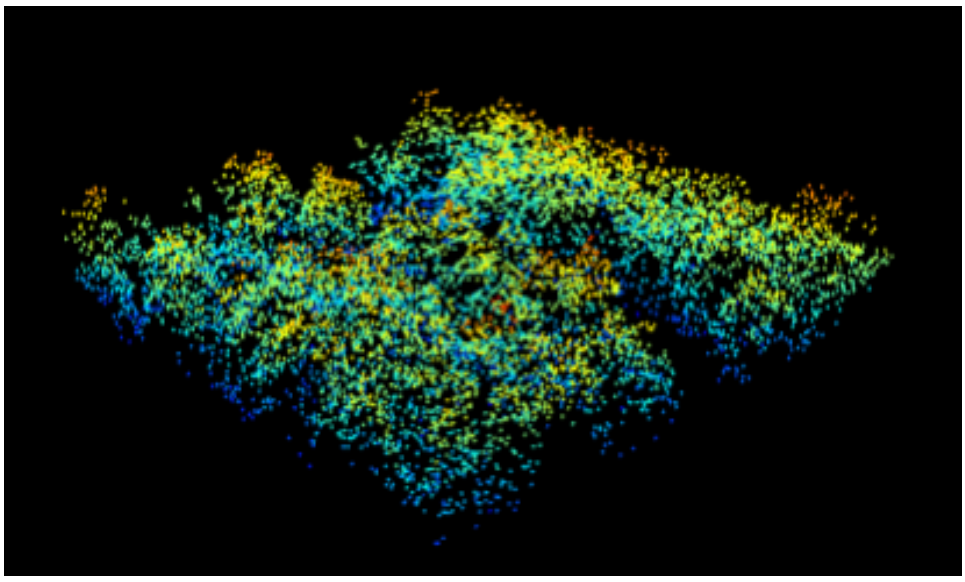

Figure 5. Sample normalized point cloud for 100m^2 forest patch, colored by height.

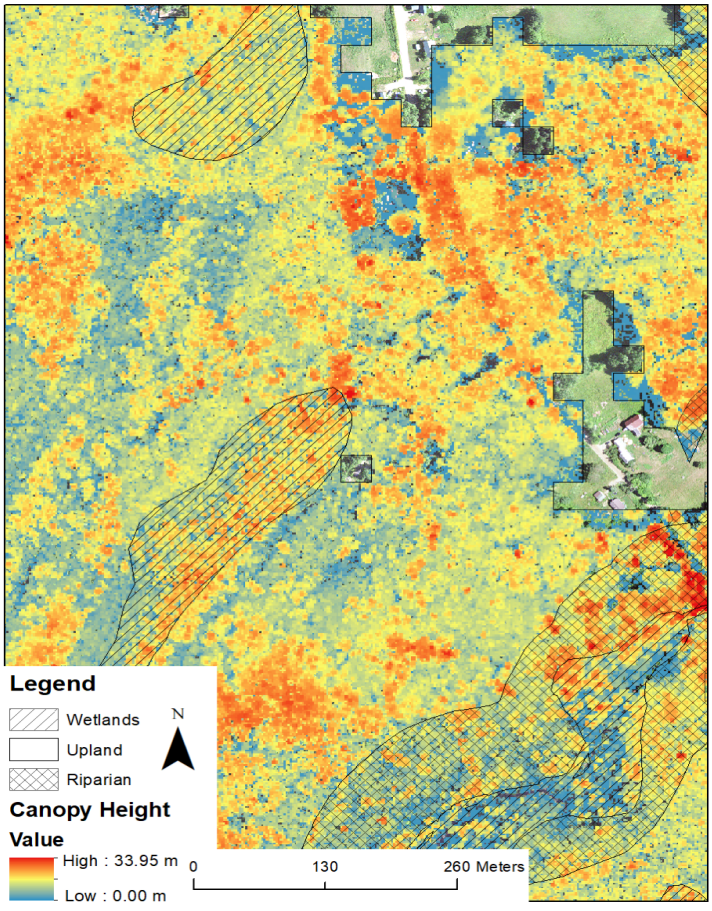

Figure 6. Sample canopy height model for all three

I clipped the point cloud to fit its corresponding polygon, and then saved each as a .las file. I also calculated statistics at the grid level for each resultant point cloud, using a 10-meter resolution to create six total rasters containing statistics such as 95th percentile height, entropy, and point totals. Figure 6 demonstrates a sample canopy height map.

In ArcGIS 10.6, I used the raster calculator to calculate growth by subtracting the 2007 raster from its corresponding 2012 raster for each forest type (ESRI 2019). From this intermediary, I calculated means and sums using the zonal statistics tool. I executed some final analysis in R (3.6.3), primarily to delineate quartiles for differences in canopy heights and to plot the relationship between existing forest height and new growth (Venables and Ripley 2002, Wickham 2016, Aphalo 2019, Bivand et al. 2019, Hijmans 2019, Wickham et al. 2019). To eliminate erroneous noise, I restricted this last analysis to only pixels above two meters in 2007. This excluded pixels where a tree was missed by lidar pulses in 2007, but measured in 2012. Return angle, wind, or other random means can all cause such results.

RESULTS

Error Assessment

Of the 23 control points I surveyed, 15 registered height differences with absolute values under that of the maximum horizontal margin of error of 25.0 centimeters, and 4 did not. Upon further examination, seven of those points over the potential error are unrepresentative of vertical error as a whole, since they arise from angled surfaces. These instead compare total differences, with both a vertical and horizontal component, and instead fall under the maximum total margin of error for this category. The final remaining point represented a new (in 2012) foundation built on former (in 2007) forest and thus is not valid as a control point. The sum total of the 15 vertical control points (including both positive and negative values) is 4.5 centimeters, reflecting the normal distribution of these errors and the lack of systematic bias across the datasets. I also ran

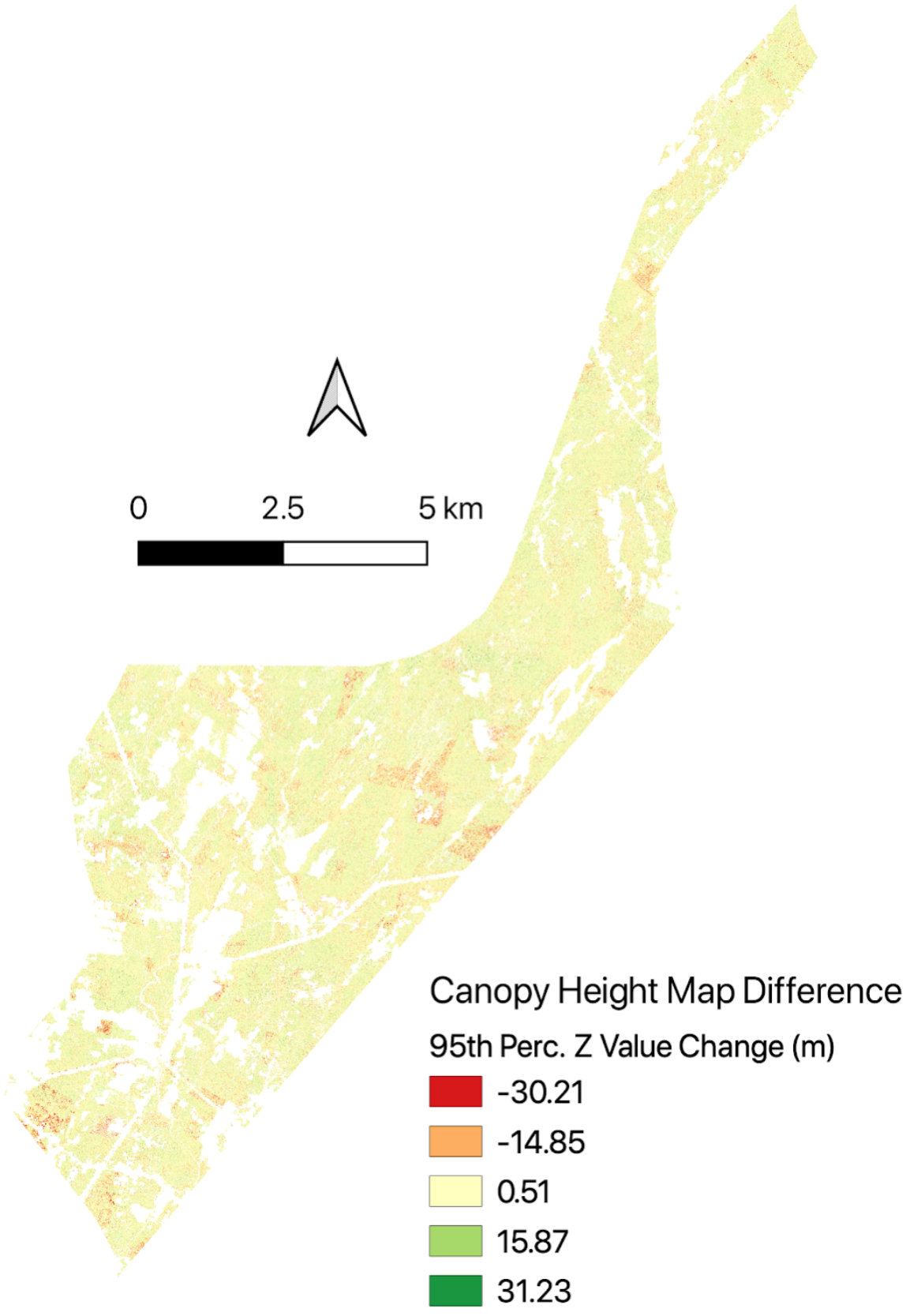

Figure 7. 95th percentile height difference map for entire study area.

1000 Monte Carlo Moran's I simulations and returned a Moran's I statistic of -0.10330 with a P value of 0.618. These values accept the null hypothesis that differences in these control points are randomly distributed, and thus I can rule out systemic error between the two datasets.

Landscape View

The final 95th percentile canopy height difference raster (showing change in forest height over the five years) is shown in Figure 7. The 95th percentile canopy height excludes the highest 5% of data points for each pixel, eliminating birds, planes, and other noise from the dataset. Additionally, this raster records absolute differences between the 2007 and 2012 canopy height maps. This offers an overall, quantitative perspective of landscape-scale forest change between 2007 and 2012. Areas of development, farm fields, and open water appear in white, and height change is recorded in green (positive) and red (negative).

Growth Difference by Forest Types

While these results do not show landscape-scale forest growth across the entire study area, certain subsets of the data show height increase in the canopy. 95th-percentile height values represent more stable estimates of canopy height than 100th-percentile values, thanks to reduced levels of noise. Across all pixels, these values record mild changes across all three forest categories (wetland, riparian, and upland), as seen in Figure 8. I recorded changes of +3.75 cm in riparian forest, +8.35 cm in wetland forest, and -1.97 cm in upland forest. Variation across these three categories is weak. By median pixel change from 2007 to 2012, riparian forest changed by +41.60 cm, wetland forest by +19.30 cm, and upland forest by +35.85 cm.

When only pixels with positive height differences are considered (i.e., only net growth from 2007 to 2012), higher growth values are recorded (Figure 9). For each category of forest, the mean growth value is roughly 140 cm, or approximately 35 centimeters per growing season. Specifically, mean upland forest grew 137.55 cm, riparian forest grew 144.14 cm, and wetland forest grew 147.01 cm. By median growth, upland forest grew 111.50 cm, riparian forest grew 117.80 cm, and wetland forest grew 147.01 cm. However, there was no significant difference across means, medians, and distributions across the three categories of forest (Figure 9). These statistics were

calculated for 361,373 pixels of upland forest, 196,692 pixels of riparian forest, and 112,072 pixels of wetland forest.

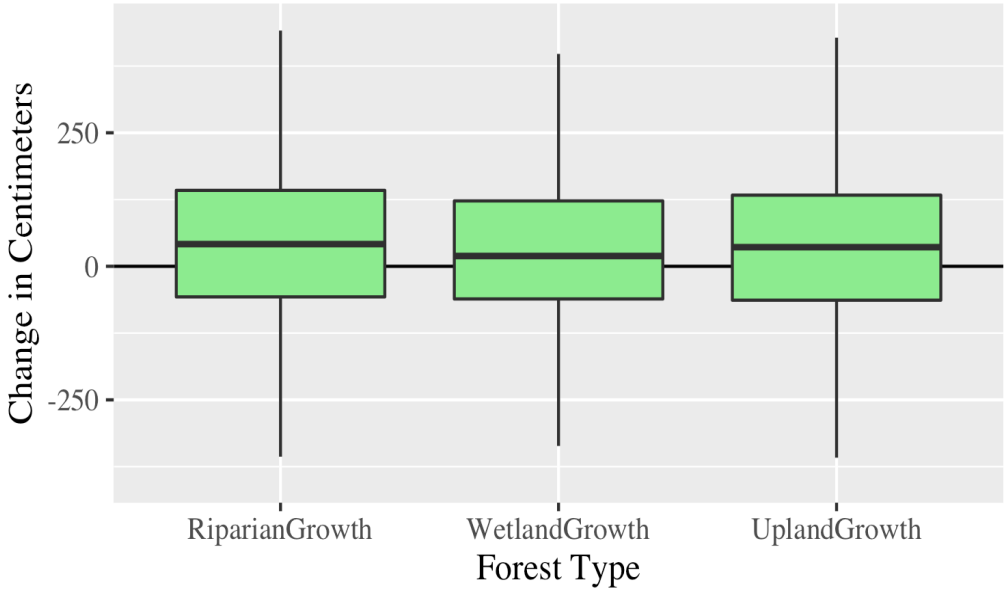

Figure 8. Distribution of All 95th Percentile Height Changes

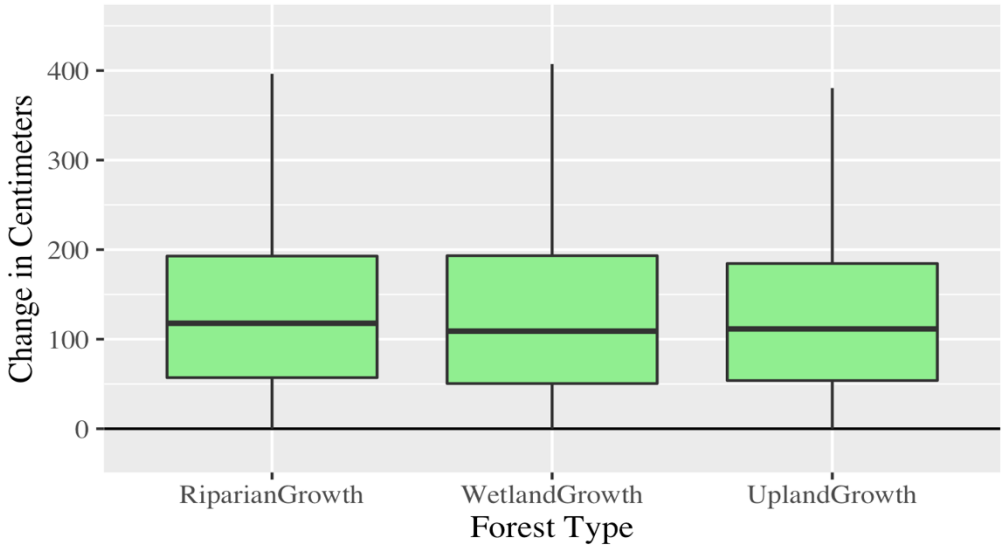

Figure 9. Distribution of positive 95th percentile height changes.

Growth Difference by Forest Height

For riparian, upland, and wetland forest, higher growth was consistently recorded in forest that was shorter in 2007 (Figure 10). In other words, taller trees in 2007 added less to their height than shorter trees. As forest height in 2007 increased, mean 95th-

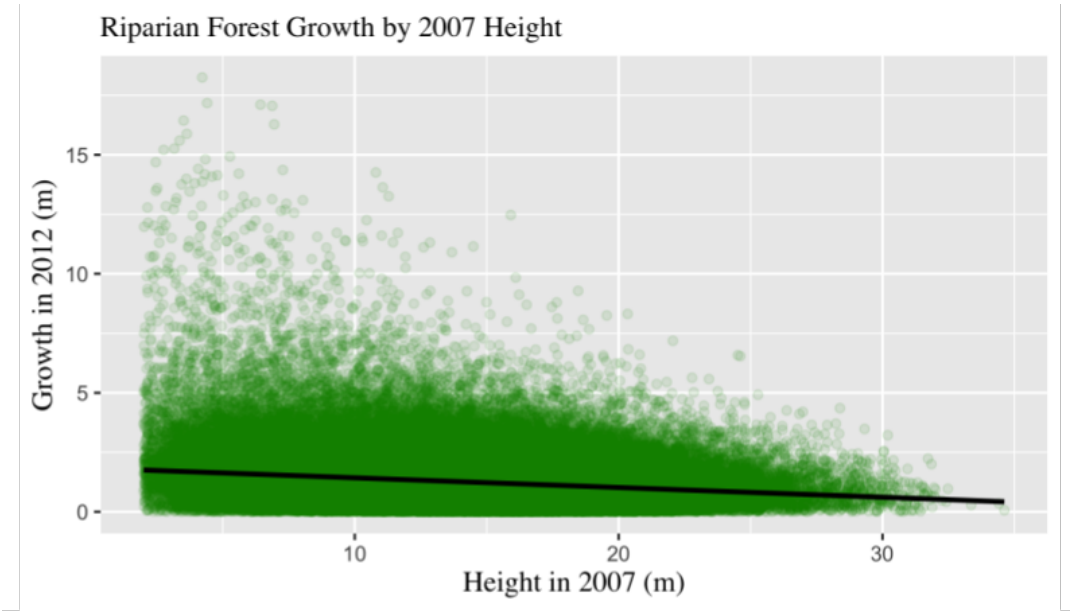

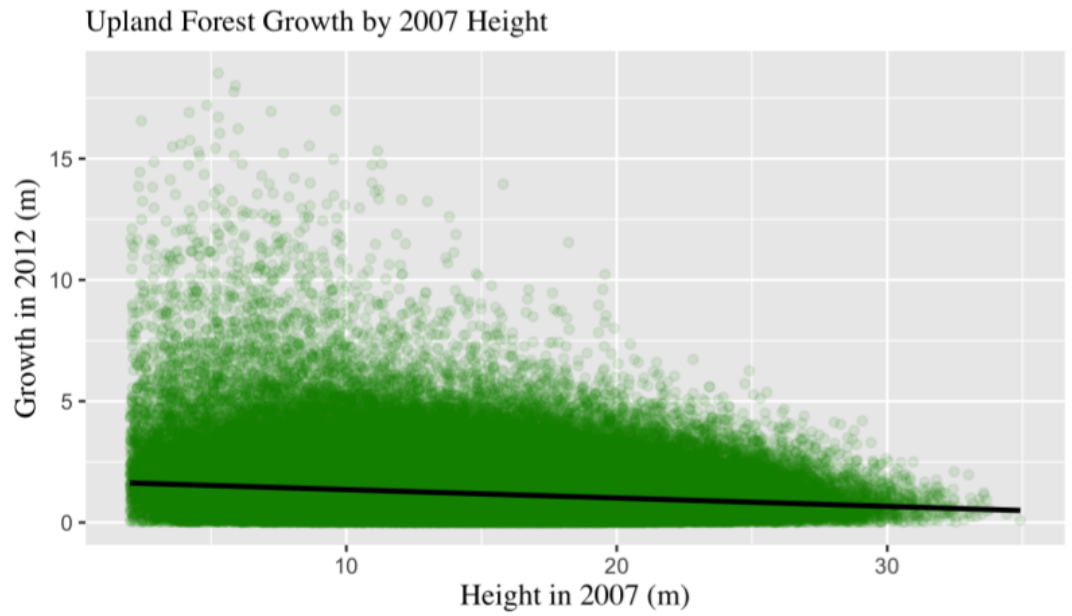

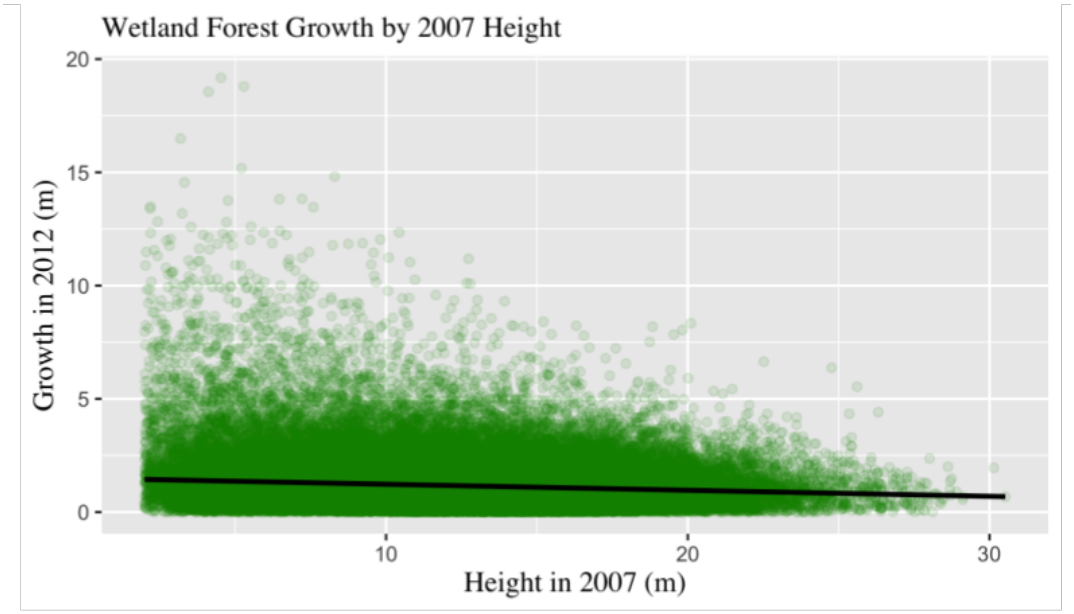

Figure 10. Forest growth by height for riparian, upland, and wetland forest.

percentile growth decreased. Again, there was no significant variation across the three categories of forest, as the standard deviation of each's bisquare regression intercepts was 0.14, or ~8% of the mean (Table 2). Riparian forest displayed a steeper curve at -0.0408 while upland (-0.0344) and wetland (-0.0266) forests possessed more gentle slopes (Table 2).

Table 2. Bisquare regression results for forest growth by height in 2007.

	Intercept	Slope	n
Riparian forest	1.836	-0.0408	115,975
Upland forest	1.700	-0.0344	207,816
Wetland forest	1.494	-0.0266	58,576

Detection of Disturbance

Forest disturbance, especially in the form of timber harvest, are readily apparent in rasters of 95th-percentile height difference (Figure 11). Additionally, height distributions derived from these areas display drastic drops in the number and density of higher-value points (Figures 12 and 13). Canopy height maps of these same areas delineate both forest harvest and skid roads used to facilitate these harvests.

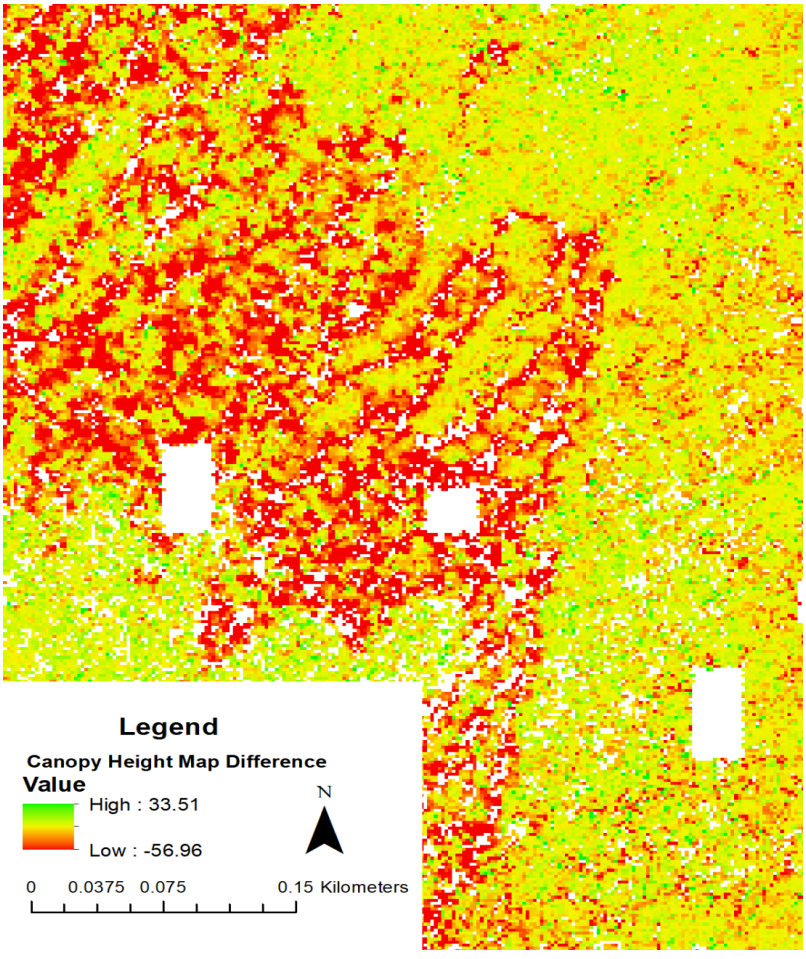

Figure 11. Harvested area (in red, left) and intact forest (in yellow-green, right) shown in canopy height difference map.

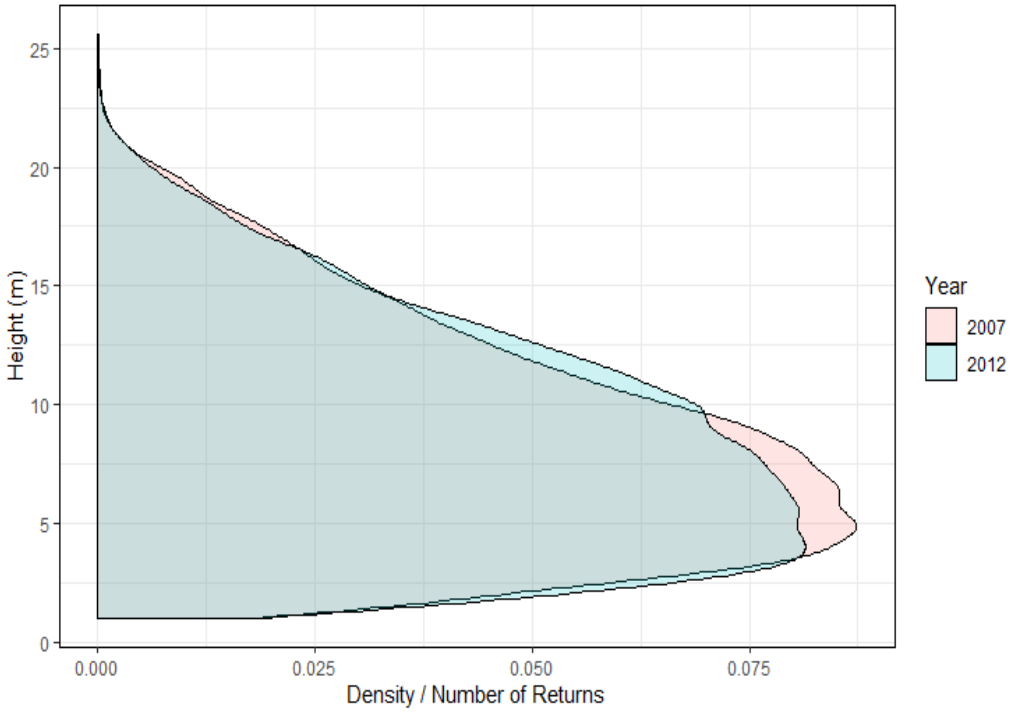

Figure 12. Return density chart for intact forest.

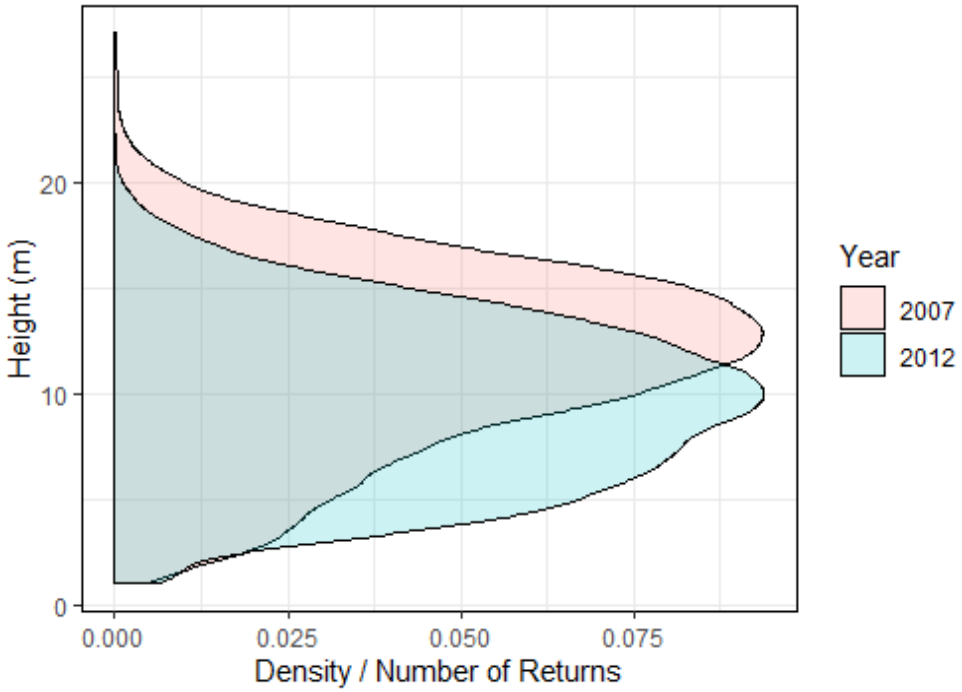

Figure 13. Return density chart for harvested forest.

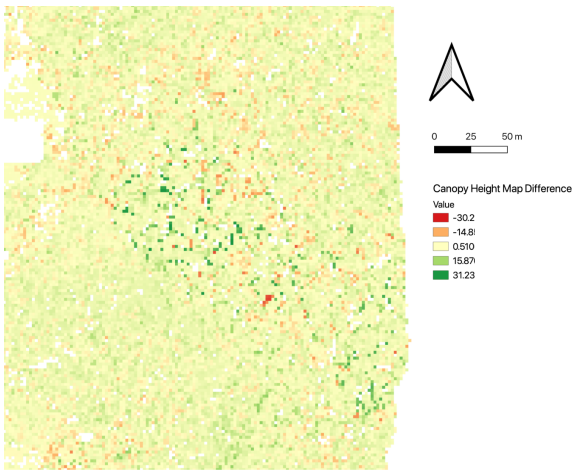

Figure 14a. Thinning, canopy height difference map.

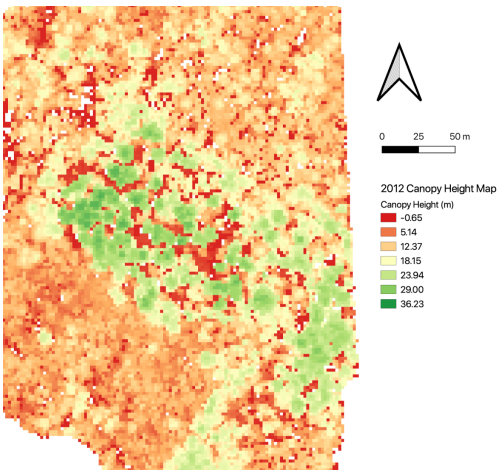

Figure 14b. Thinning, 2012 canopy height map.

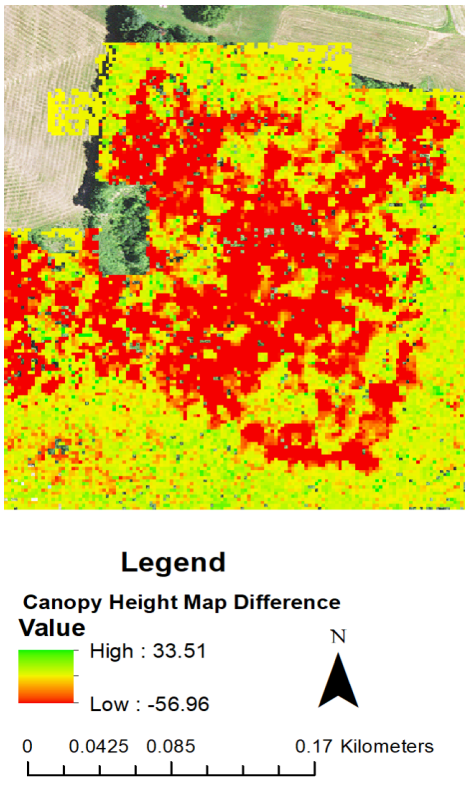

Figure 15. Clearcut.

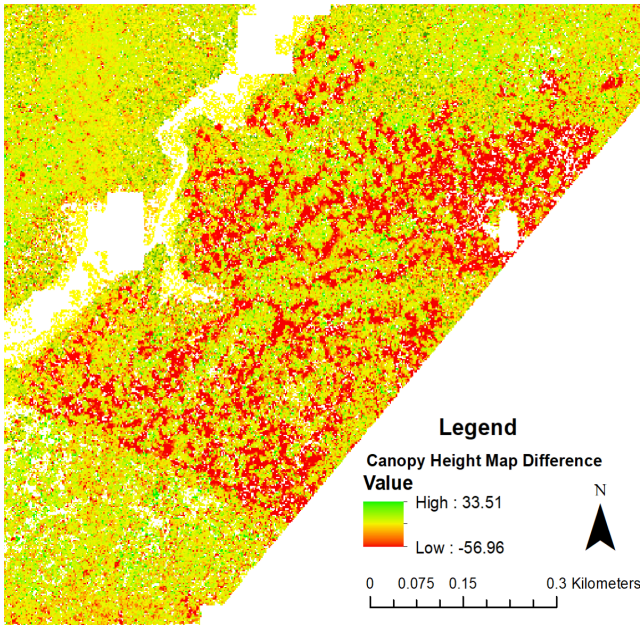

Figure 16. Selective harvest.

Forest Management Approaches

In some cases, though not all, specific forest management approaches are discernable from the 95th-percentile difference rasters. In one area of particularly high

growth, thinning is evident (Figures 14a and 14b). Clearcuts are also apparent in Figure 15. Finally, selective harvests are especially demonstrable, as in Figure 16.

DISCUSSION

Harvest Patterns

This landscape-scale analysis of bitemporal lidar describes broad patterns of forest harvest as well as patterns of forest growth, a result of south-central Maine's pattern of land ownership and development practices. Trends in 95th percentile height growth, for instance, indicate near-stasis in terms of net canopy change. Since central Maine largely lacks slow-growing old-growth forest, this could indicate that harvests nearly cancel out each year's growth. In other words, biomass extracted from these forests is nearly equal to the biomass added each year.

95th percentile forest heights should not naturally decline year-over-year, except in rare cases such as large storm events and forest fires (Lorimer 1977, Smith and Shortle 2003). By considering only instances of height growth, as opposed to height loss, I hoped to more accurately capture growth rates as a whole by excluding harvested areas. However, none of these growth rates (each around 33-38 centimeters per year) align with existing estimates of growth of roughly 60 centimeters per year (Dolan et al. 2009). This is potentially explained by irregular forest patches left behind by partial harvests, which could skew the remaining positive pixels.

I analyzed this trend in further detail by comparing each pixel's growth (from 2007 to 2012) to its starting height in 2007. For riparian, upland, and wetland forest, forest growth rate was inversely related to starting height (Figure 7). This matches the well-known property of stand development that growth rates decline as the forest canopy closes (Gower et al. 1996, Ryan et al. 1997). These data also explain why the observed growth rates are substantially lower than the idealized growth rates observed by Dolan et al. (2009). Though the lines of best fit for these three forest types show no significant differences, wetland forest displayed the steepest curve, followed by riparian and upland forest. This indicates that growth (at least vertically) declines more rapidly with height in wetlands than in other forests. This potentially reflects lower nutrient levels in bog and peatland environments and lower overall heights (Damman 1978, Damman 1988).

Differential Growth

This study revealed no strong patterns between wetland, riparian, and upland forest. 95th percentile height data, positive 95th percentile height data, and trends in growth versus existing height showed similar data across the three forest categories. Mean 95th percentile canopy heights, for both all and only positive data, varied especially little in comparison to the distribution of values (Figures 5 and 6). There are several potential explanations for these similarities. First, growth patterns amongst these three categories of forest may indeed be very similar. This seems unlikely due to known differences in nutrient availability and species distributions (Niswander and Mitsch 1995, Ricker et al. 2013). Second, the point clouds may lack the requisite density or accuracy to show differences at the scale of forest category. This too seems unlikely, given the results of error assessment and the overall growth estimates detailed earlier.

Two more potential explanations seem most likely in explaining the lack of variation amongst categories. The first lies with the physical delineation of each category. For the sake of consistency, time, and computational practicality, I used data from the National Wetlands Inventory for wetlands and streamlines (from which riparian forest were delineated). Though largely accurate, these datasets cannot be groundtruthed to complete accuracy, and may contain some errors (Kudray and Gale 2000). Additionally, though I restricted wetlands to only those with greater than 50% forest cover, it is possible that some non-forested was inadvertently included in the final polygon due to error in the NLCD raster. The final potential explanation for the lack of variation in growth patterns lies with other factors in forest growth. Soil type, aspect, land use history, and various other factors may combine to play a more important role in determining how quickly a forest's canopy grows.

Forest Management

Despite the lack of strong patterns between the three forest types, this study showed lidar can support forest monitoring and conditions, even with two datasets created for disparate uses. While natural growth in intact forest was difficult to untangle, human impacts over five years was simple to detect. The data illustrates the stark visibility of harvest in both height maps and vertical profiles (Figures 8, 9, 10), as well as different types of forest management regimes (Figures 11, 12, 13). While classifying

thinning, selective harvest, and clearcuts with these data requires manual identification, their identification is still possible with point densities below 3 pts/m^2 in leaf-off conditions.

Bitemporal lidar's ability to detect different forest management styles (or at least harvest) imply a broader use for large-scale forest monitoring. Other researchers have proposed or accomplished similar levels of monitoring using Landsat data (Wilson and Sader 2002, Hermosilla et al. 2016). In Maine forests, Pangaribuan and Sader (1997) were able to use satellite imagery to delineate different forest management styles across three time steps. However, beyond the simple presence and classification of forestry methods, lidar could facilitate rough estimates of canopy height change, approximate age of harvested forest, and biomass loss (Englhart et al. 2013, Cao et al. 2016, Becknell et al. 2018). Past attempts to monitor these statistics over large-scales have also included self-reporting on the part of the harvester as well as cooperative monitoring (Pokorny and Steinbrenner 2005, Wilkinson et al. 2014). In Maine, a combination of classified Landsat imagery, sampled high-resolution imagery, and selected ground measurements are used to monitor the Pingree Conservation Easement, consisting of roughly 3,075 km^2 of forestland (Sader et al. 2002). Lidar holds several advantages over these in-person sampling methods. Lidar can enable landscape-level monitoring, without reducing data points to random samples. Additionally, surveys can be performed without obstruction on the part of an unwilling harvester or landowner. As such, bi- and multi-temporal lidar surveys offer considerable potential for forest monitoring, as demonstrated by this study.

Study Limitations

As with all large-scale remote sensing projects, there are considerable sources of error that could potentially have limited observations and affected the final results. Underlying seasonal differences between the 2007 (autumn) and 2012 (spring) datasets could have led to fundamentally different z-value distributions. For instance, marcescent trees like American beech and northern red oak retain their leaves through winter but not spring (Addicott, 1982). Additionally, since both datasets were recorded in largely leaf-off conditions, overall above-ground point densities were reduced. More laser pulses simply hit the ground instead of trees. This especially restricted the ability to detect understory growth. There are also inherent limitations to the classification of different

forest types. Ground-truthing the National Wetland Inventory's classification of wetlands or the National Hydrography Dataset's stream flowlines was impractical and time-costly. Similarly, the National Land Cover Database's classification of forest cover derives data from 2016 and thus may not fully describe either the 2007 or the 2012 datasets. Additionally, the forest cover cutoff (50%, in this study) imperfectly fit the study area in terms of including undeveloped forest and excluding manmade structures. Though largely effective and incredibly valuable, these simplifications led to imperfections in these datasets have the potential to affect the accuracy of the final product.

On the processing side, the resolution of the metrics output raster was unfortunately restricted to 10 meters due to limited computational memory. Though detailed for landscape- and parcel-level analysis, this approach is too coarse to delineate individual trees. This, in combination with the low point density of the 2012 dataset, prevented effective quantitative analysis of individual trees.

Future Study

As I have shown in this study, bitemporal analysis of lidar point clouds facilitates characterization of forest canopy height change, as well as forest management style. Though far from abundant, overlapping lidar datasets exist elsewhere in New England and warrant investigation. Two regions in Maine in particular (the headwaters of the Narragaugus and Pleasant Rivers) contain intersecting datasets. Since one of these datasets is from the same study as the 2007 dataset utilized here and the other are datasets compiled by the Maine Office of GIS, these comparisons could be performed very similarly to this one.

As airborne lidar becomes cheaper and more commonly utilized, overlapping datasets will increase in both quantity and quality. This should facilitate further forest growth comparisons across various categories not considered here, such as soils, land ownership, or gradient. In concert with other sources of data, such as high-resolution aerial imagery, future researchers may compare growth variance across different forest communities as well. Future studies could also develop algorithms and automated schemes for classifying forest management types with lidar.

CONCLUSIONS

Bitemporal forest comparison and analysis is indeed possible in datasets created for disparate purposes. Though differences in growth between wetland, riparian, and upland forests are difficult to distinguish, overall canopy growth generally aligns with expected rates. Additionally, this study shows that lidar-detected canopy growth is inversely related to initial canopy height. Finally, this analysis allows manual identification of different types of forest management, like thinning, selective harvest, and clearcutting as well as its impact on canopy height.

However, data accuracy is limited to the least accurate dataset at best, and the sum of both datasets' error at worst. Additionally, seasonal constraints may limit the utility of forest comparison by restricting evidence of understory. Even with these current limitations in mind, the future remains bright. As data quality and quantity improves throughout Maine and the United States, the value of lidar as an efficient, accurate temporal tool will only grow.

REFERENCES

Addicott, F. 1982. Abscission. University of California Press. Berkeley, USA.

Aphalo, P. 2019. ggpmisc: Miscellaneous Extensions to 'ggplot2'. R package version 0.3.3. https://CRAN.R-project.org/package=ggpmisc

Asner, G., J. Mascaro, H. Muller-Landau, G. Vieilledent, R. Vaudry, M. Rasamoelina, J. Hall, and M. van Breugel. 2012. A universal airborne LiDAR approach for tropical forest carbon mapping. Oecologia **168**:1147-1160.

Becknell, J., S. Porder, S. Hancock, R. Chazdon, M. Hofton, J. Blair, & J. Kellner. 2018. Chronosequence predictions are robust in a Neotropical secondary forest, but plots miss the mark. Global Change Biology **24**:933-943.

Beland, M., G. Parker, B. Sparrow, D. Harding, L. Chasmer, S. Phinn, A. Antonarakis, and A. Strahler. 2019. On promoting the use of lidar systems in forest ecosystem research. Forest Ecology and Management **450**:117484.

Bivand, R., E. Pebesma, and V. Gomez-Rubio. 2013. Applied Spatial Data Analysis with R, Second edition. Springer, NY. http://www.asdar-book.org/

Bivand, R., T. Keitt and B. Rowlingson. 2019. rgdal: Bindings for the 'Geospatial' Data Abstraction Library. R package version 1.4-8. https://CRAN.R-project.org/package=rgdal

Bromley, S. 1935. The original forest types of southern New England. Ecological Monographs **5**:61-89.

Brooks, R. and T. Kyker-Snowman. 2009. Forest-floor temperatures and soil moisture across riparian zones on first- to third-order headwater streams in southern New England, USA. Forest Ecology and Management **258**:2117-2126.

Campell, J., J. Hornbeck, W. McDowell, D. Buso, J. Shanley, and G. Likens. 2000. Dissolved organic nitrogen budgets for upland, forested ecosystems in New England. Biogeochemistry **49**:123-142.

Cao L., N. Coops, J. Innes, S. Sheppard, L. Fu, H. Ruan, G. She. 2016. Estimation of forest biomass dynamics in subtropical forests using multi-temporal airborne LiDAR data. Remote Sensing of Environment. **178**:158-171.

Chen, J., S. Saunders, T. Crow, R. Naiman, K. Brosofske, G. Mroz, B. Brookshire, and J. Franklin. 1999. Microclimate in forest ecosystem and landscape ecology: variations in local climate can be used to monitor and compare the effects of different management regimes. BioScience **49**:288-297.

Coops, N., T. Hilker, M. Wulder, B. St-Onge, G. Newnham, A. Siggins, and J. Trofymow. 2007. Estimating canopy structure of Douglas-fir forest stands from discrete-return LiDAR. Trees **21**:295-310.

Copenheaver, C., A. White, and W. Patterson. 2000. Vegetation development in a southern Maine pitch pine-scrub oak barren. Journal of the Torrey Botanical Society **127**:19-32.

Dammon, A. 1978. Distribution and movement of elements in ombrotrophic peat bogs. Oikos **30**:480-495.

Damman, A. 1988. Regulation of nitrogen removal and retention in sphagnum bogs and other peatlands. Oikos **51**:291-305.

Dassot, M., T. Constant, and M. Fournier. 2011. The use of terrestrial LiDAR technology in forest science: application fields, benefits and challenges. Annals of Forest Science **68**:959-974.

Dolan, K., J. Masek, C. Huang, and G. Sun. 2009. Regional forest growth rates measured by combining ICESat GLAS and Landsat data. Journal of Geophysical Research **114**:G00E05.

Eitel, J., B. Höfle, L. Vierling, A. Abellán, G. Asner, J. Deems, C. Glennie, P. Joerg, A. LeWinter, T. Magney, G. Mandlburger, D. Morton, J. Müller, and K. Vierling. 2016. Beyond 3-D: The new spectrum of lidar applications for earth and ecological sciences. Remote Sensing of Environment **186**:372-392.

Englhart, S., J. Jubanski, F. Siegert. 2013. Quantifying dynamics in tropical peat swamp forest biomass with multi-temporal LiDAR datasets. Remote Sensing: **5**:2368-2388.

ESRI 2019. ArcGIS Desktop: Release 10.6. Redlands, CA: Environmental Systems Research Institute.

Farrell, S., B. Collier, K. Skow, A. Long, A. Campomizzi, M. Morrison, K. Hays, and R. Wilkins. 2013. Using LiDAR-derived vegetation metrics for high-resolution, species distribution models for conservation planning. Ecosphere **4**(3):42.

Hijmans, R.. 2019. raster: Geographic Data Analysis and Modeling. R package version 3.0-7. https://CRAN.R-project.org/package=raster

Gawler, S. and A. Cutko. 2018. Natural Landscapes of Maine. Maine Natural Areas Program, Augusta.

Gilmore, M., E. Wilson, N. Barrett, D. Civco, S. Prisloe, J. Hurd, and C. Chadwick. 2008. Integrating multi-temporal spectral and structural information to map

wetland vegetation in a lower Connecticut River tidal marsh. Remote Sensing of Environment **112**:4048-4060.

Gotelli, N., P. Mouser, S. Hudman, S. Morales, D. Ross, and A. Ellison. 2008. Geographic variation in nutrient availability, stoichiometry, and metal concentrations of plants and pore-water in ombrotrophic bogs in New England, USA. Wetlands **28**:827-840.

Gower, S., R. McMurtrie, D. Murty. 1996. Aboveground net primary production decline with stand age: potential causes. Trends in Ecology & Evolution **11**:378-382.

Hawes, E., and M. Smith. 2005. Riparian Buffer Zones: Functions and Recommended Widths. Eightmile River Wild and Scenic Study Committee.

Hayashi, R., A. Weiskittel, S. Sader. 2014. Assessing the feasibility of low-density LiDAR for stand inventory attribute predictions in complex and managed forests of northern Maine, USA. Forests **5**:363-383.

Hermosilla, T., M. Wulder, J. White, N. Coops, G. Hobart, L. Campbell. 2016. Mass data processing of time series Landsat imagery: pixels to data products for forest monitoring. International Journal of Digital Earth **9**:1035-1054.

Khosravipour, A., A. Skidmore, M. Isenburg, T. Wang, and Y. Hussin. 2014. Generating pit-free canopy height models from airborne lidar. Photogrammetric Engineering & Remote Sensing **80**:863-872.

Kudray, G. and M. Gale. 2000. Evaluation of National Wetland Inventory maps in a heavily forested region in the upper Great Lakes. Wetlands **20**:581-587.

Laser, M., J. Jorden, and K. Nislow. 2009. Riparian forest and instream large wood characteristics, West Branch Sheepscot River, Maine, USA. Forest Ecology and Management **257**:1558-1565.

Lim, K., P. Treitz, M. Wulder, B. St-Onge, and M. Flood. 2003. LiDAR remote sensing of forest structure. Progress in Physical Geography: Earth and Environment **27**:88-106.

Lim, K., P. Treitz, K. Baldwin, I. Morrison, and J. Green. 2014. Lidar remote sensing of biophysical properties of tolerant northern hardwood forests. Canadian Journal of Remote Sensing **29**:658-678.

Lorimer, C. 1977. The presettlement forest and natural disturbance cycle of Northeastern Maine. Ecology **58:**139-148.

Lovell, J., D. Jupp, G. Newnham, N. Coops, and D. Culvenor. 2005. Simulation study for finding optimal lidar acquisition parameters for forest height retrieval. Forest Ecology and Management **214**:398-412.

Ma, Q., Y. Su, S. Tao, and Q. Guo. 2017. Quantifying individual tree growth and tree competition using bi-temporal airborne laser scanning data: a case study in the Sierra Nevada Mountains, California. International Journal of Digital Earth **11**:485-503.

Maine Forest Service, Department of Conservation. 2010. Maine State Forest Assessment and Strategies. Maine Forest Service, Department of Conservation, Augusta.

McGlynn, B., J. McDonnell, J. Shanley, and C. Kendall. 1999. Riparian zone flowpath dynamics during snowmelt in a small headwater catchment. Journal of Hydrology **222**:75-92.

McLean, J., L. Sewall, L. Pugh. 2007. Sheepscot River Watershed Management Plan. Time & Tide Resource Conservation & Development Area, Augusta, Maine.

McKinney, R. and M. Charpentier. 2009. Extent, properties, and landscape setting of geographically isolated wetlands in urban southern New England watersheds. Wetlands Ecology and Management **17**:331-344.

McWilliams, W., B. Butler, D. Griffith, M. Hoppus, A. Lister, T. Lister, R. Morin, L. Steward, J. Westfall, J. Steinman, C. Woodall, L. Caldwell, K. Laustsen, S. Sader, J. Metzler, D. Williams, and A. Whitman. 2004. The Forests of Maine: 2003. The Forests of Maine: 2003. Northeastern Research Station, Newtown Square, PA.

Michez, A., H. Piégay, J. Lisein, H. Claessens, and P. Lejeune. 2016. Classification of riparian forest species and health condition using multi-temporal and hyperspatial imagery from unmanned aerial system. Environmental Monitoring and Assessment **188**:146.

Niswander, S. and W. Mitsch. 1995. Functional analysis of a two-year-old created in-stream wetland: hydrology, phosphorus retention, and vegetation survival and growth. Wetlands **15**:212-225.

OCM Partners, 2020: 2012 MEGIS Topographic Lidar: Statewide Lidar Project Areas 2 and 3 (Mid-Coastal Cleanup), Maine, https://inport.nmfs.noaa.gov/inport/item/49791.

Ohmann, L. and D. Grigal. 1985. Biomass distribution of unmanaged upland forests in Minnesota. Forest Ecology and Management **13**:205-222.

Pangaribuan, H. and S. Sader. 1997. Evaluation of satellite change detection methods for monitoring forest harvest and silvicultural activity in Maine industrial forests.

Proceedings of the Society of Photo-Optical Instrumentation Engineers 3119, Multispectral Imaging for Terrestrial Applications II.

Pokorny, B. and M. Steinbrenner. 2005. Collaborative monitoring of production and costs of timber harvest operations in the Brazilian Amazon. Ecology and Society **10**:3-23.

R Core Team 2019. R: A Language and Environment for Statistical Computing. R Foundation for Statistical Computing, Vienna, Austria. https://www.R-project.org/.

Ricker, M., M. Stolt, S. Donohue, G. Blazejewski, and M. Zavada. 2013. Soil organic carbon pools in riparian landscapes of southern New England. Soil Science Society of America Journal **77**:1070-1079.

Roussel, J., and D. Auty 2020. lidR: Airborne LiDAR Data Manipulation and Visualization for Forestry Applications. R package version 2.0.0. https://CRAN.R-project.org/package=lidR

Ryan, M., D. Binkley, and J. Fownes. 1997. Age-related decline in forest productivity: pattern and process. Advances in Ecological Research **27**:213-262

Sader, S., K. Ross, and F. Reed. 2002. Pingree Forest Partnership: monitoring easements at the landscape level. Journal of Forestry **99**:18-25.

Smith, K., and W. Shortle. 2003. Radial growth of hardwoods following the 1998 ice storm in New Hampshire and Maine. Canadian Journal of Forest Research **33**:325-329.

Snyder, N. 2013. Survey of Sheepscot, Narragaugus and Pleasant Rivers, Maine. http://opentopo.sdsc.edu/datasetMetadata?otCollectionID=OT.042013.26919.1.

Sumnall, M., A. Peduzzi, T.R. Fox, R.H. Wynne, and V.A. Thomas. 2016. Analysis of a lidar voxel-derived vertical profile at the plot and individual tree scales for the estimation of forest canopy layer characteristics. International Journal of Remote Sensing 37:2653-2681.

Toledo, M., L. Poorter, M. Peña-Claros, A. Alarcón, J. Balcázar, C. Leaño, J. Licona, O. Llanque, V. Vroomans, P. Zuidema, and F. Bongers. 2010. Climate is a stronger driver of tree and forest growth rates than soil and disturbance. Journal of Ecology **99**:254-264.

van Ewijk, K., P. Treitz, & N. Scott. 2011. Characterizing forest succession in central Ontario using LAS-derived indices. Photogrammetric Engineering and Remote Sensing, **77**:261-269

van Leeuwen, M., and M. Nieuwenhuis. 2010. Retrieval of forest structural parameters using LiDAR remote sensing. European Journal of Forest Research **129**:749-770.

Vastaranta, M., I. Korpela, A. Uotila, A. Hovi, and M. Holopainen. 2012. Mapping of snow-damaged trees based on bitemporal airborne LiDAR data. European Journal of Forest Research **131**:1217-1228

Venables, W., and B. Ripley. 2002. Modern Applied Statistics with S. Fourth Edition. R package version 7.3-51.5. Springer, New York.

Ventura, G., G. Vilardo, C. Terranova, and E. Bellucci Sessa. 2011. Tracking and evolution of complex active landslides by multi-temporal airborne LiDAR data: The Montaguto landslide (Southern Italy). Remote Sensing of Environment **115**:3237-3248.

Vepakomma, U., B. St-Onge, and D. Kneeshaw. 2008. Spatially explicit characterization of boreal forest gap dynamics using multi-temporal lidar data. Remote Sensing of Environment **112**:2326-2340.

Vepakomma, U., D. Kneeshaw, and B. St-Onge. 2010. Interactions of multiple disturbances in shaping boreal forest dynamics: a spatially explicit analysis using multi-temporal lidar data and high-resolution imagery. Journal of Ecology **98**:526-539.

Wickham, H. ggplot2: Elegant Graphics for Data Analysis. R package version 3.2.1. Springer-Verlag New York, 2016.

Wickham, H., M. Averick, J. Bryan, W. Chang, L. D'Agostino McGowan, R. François, G. Grolemund, A. Hayes, L. Henry, J. Hester, M. Kuhn, T. Lin Pedersen, E. Miller, S. Milton Bache, K. Müller, J. Ooms, D. Robinson, D. Seidel, V. Spinu, K. Takahashi, D. Vaughan, C. Wilke, K. Woo, and H. Yutani (2019). Welcome to the tidyverse. Journal of Open Source Software **4**:1686.

Wilkenson, G., M. Schofield, and P. Kanowski. 2014. Regulating forestry - experience with compliance and enforcement over the 25 years of Tanzania's forest practices system. Forest Policy and Economics **40**:1-11.

Wilson, E., and S. Sader. 2002. Detection of forest harvest type using multiple dates of Landsat™ imagery. Remote Sensing of Environment **80**:385-396.

Wulder, M., J. White, F. Alvarez, T. Han, J. Rogan, and B. Hawkes. 2009. Characterizing boreal forest wildfire with multi-temporal Landsat and LIDAR data. Remote Sensing of Environment **113**:1540-1555.

Zhao, K., J. Suarez, M. Garcia, T. Hu, C. Wang, and A. Londo. 2018. Utility of multitemporal lidar for forest and carbon monitoring: Tree growth, biomass dynamics, and carbon flux. Remote Sensing of Environment **204**:883-897.

APPENDICES

Appendix I

Control points and associated metadata, as well as vertical density curves with peaks.

Control Points and Differences in Z Value Density Peaks

Control Point	Dec. Deg. Coordinates	Description	Area (m^2)	Difference in cm (2012-2007)
1	44.309792, -69.578159	angled roof	3458.1	74.6
2	44.309792, -69.578159	parking lot	3458.1	4.9
3	44.30665, -69.551666	angled roof	2240.4	-16.1
4	44.30665, -69.551666	parking lot	2240.4	13.3
5	44.395057,-69.47024	angled roof	123.3	-32.3
6	44.31211, -69.536657	swimming pool	168.3	-9.2
7	44.282475,-69.595668	flat roof	346.0	1.6
8	44.266698,-69.564562	bridge deck	294.5	8.6
9	N/A	cleared forest	N/A	N/A
10	44.323839, -69.582665	angled roof	50.3	34.5
11	44.387664,-69.467312	flat roof	146.5	-2.4
12	44.398542,-69.470484	parking lot	1080.8	-21.4
13	44.333097,-69.562786	flat roof	58.8	3.5
14	44.335838,-69.568091	bridge deck	38.7	12.6
15	44.334468,-69.546692	intersection	81.0	-11.6
16	44.306265,-69.556929	bridge deck	118.7	4.5
17	44.310839,-69.537796	flat roof	37.7	-9.7
18	44.290022,-69.565096	bridge deck	36.8	-2.7
19	44.274679,-69.570092	intersection	145.3	0.8
20	44.368234,-69.469979	road surface	101.4	1.6

21	44.333947,-69.495806	road surface	146.7	4.4
22	44.308511,-69.507611	road surface	142.4	21.8
23	44.423831,-69.439007	parking lot	360.3	0.4

Control Points and Density Curves

1	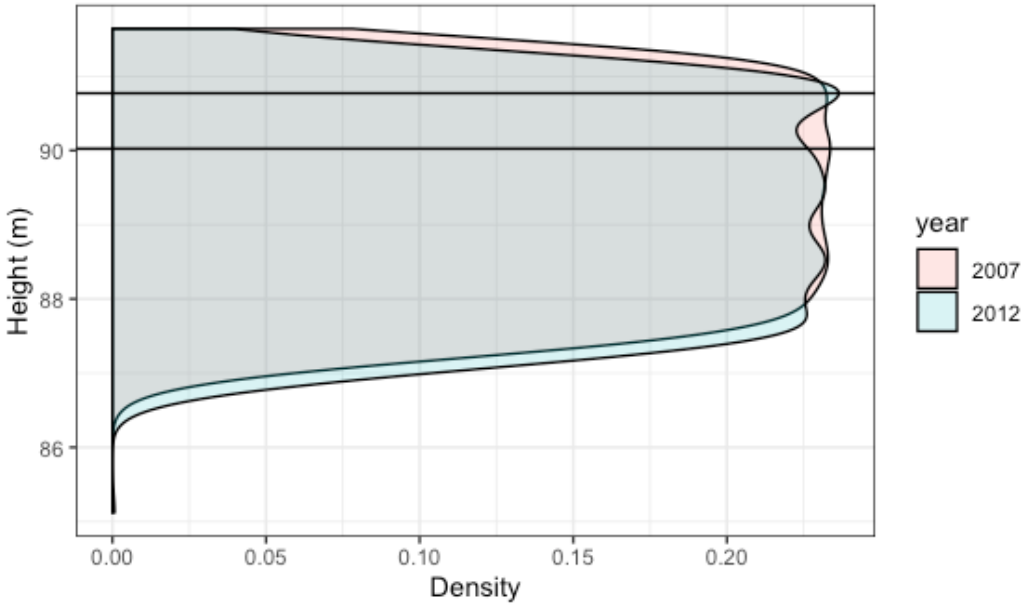
2	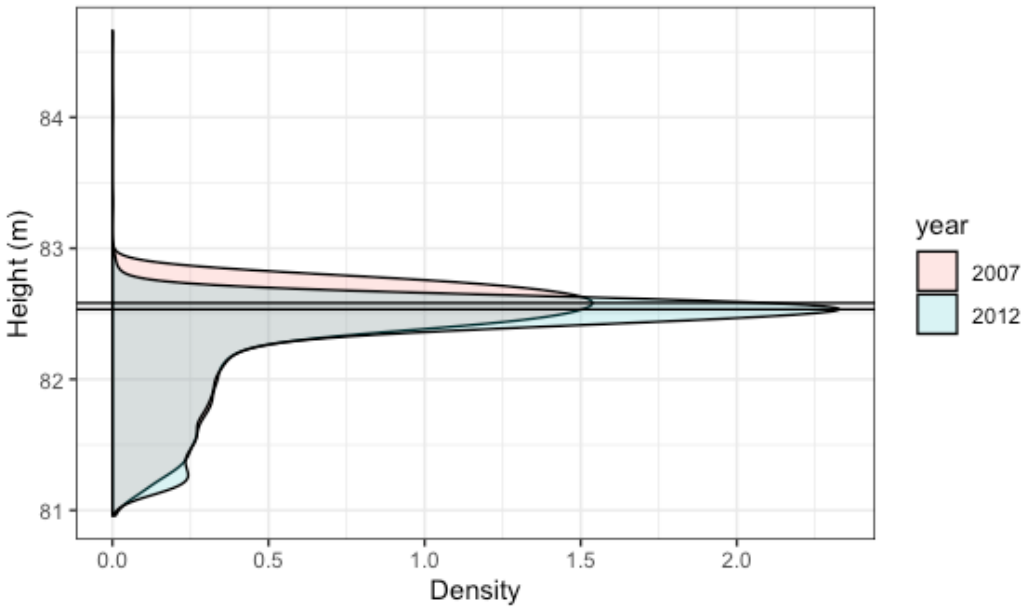

3

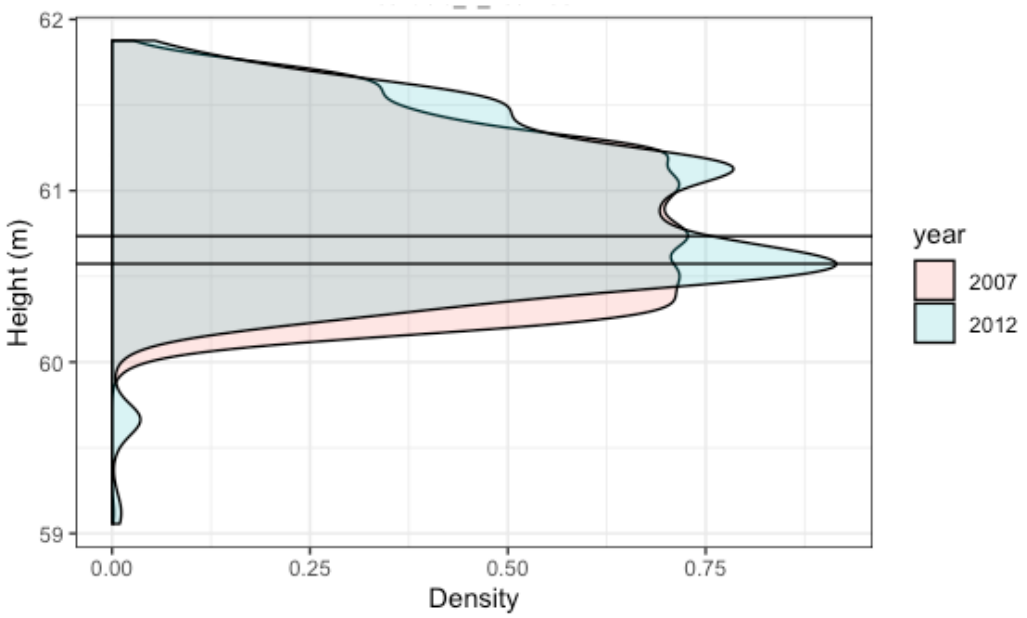
62
61
60
59
Height (m)
0.00
0.25
0.50
0.75
Density
year
2007
2012

4

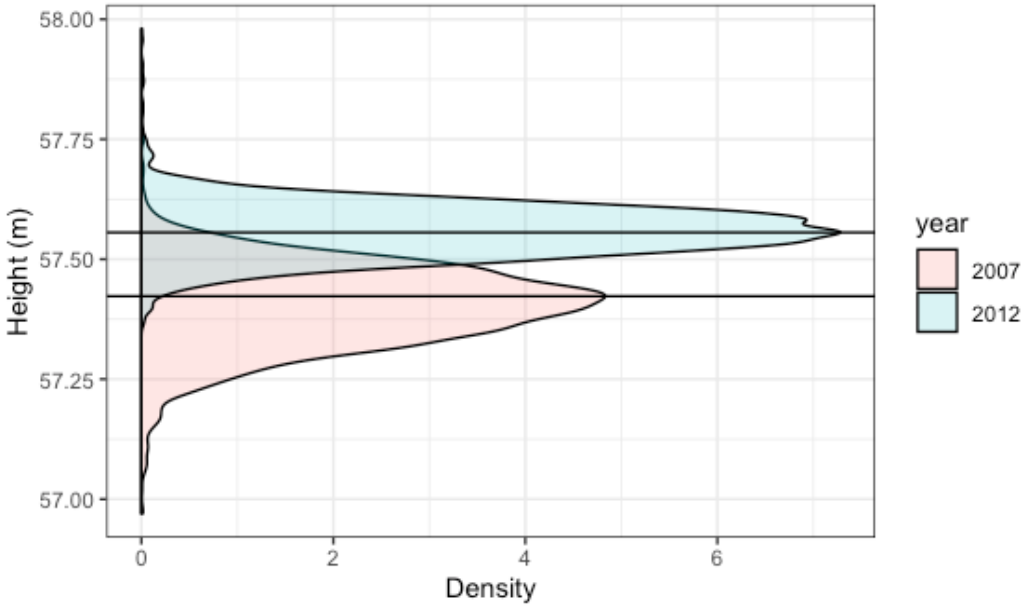
58.00
57.75
57.50
57.25
57.00
Height (m)
0
2
4
6
Density
year
2007
2012

5

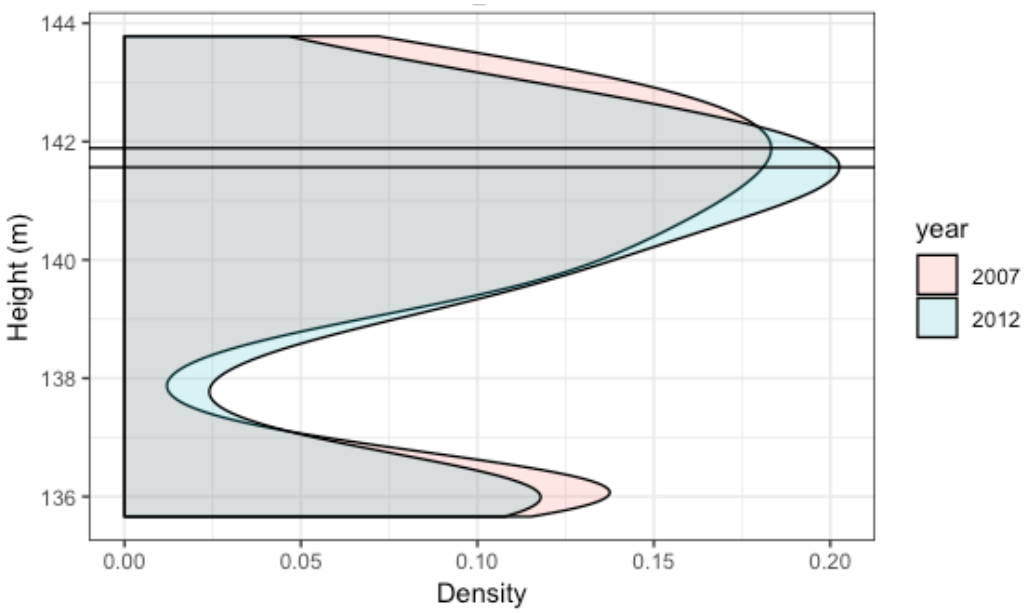
144
142
140
138
136
Height (m)
0.00
0.05
0.10
0.15
0.20
Density
year
2007
2012

6

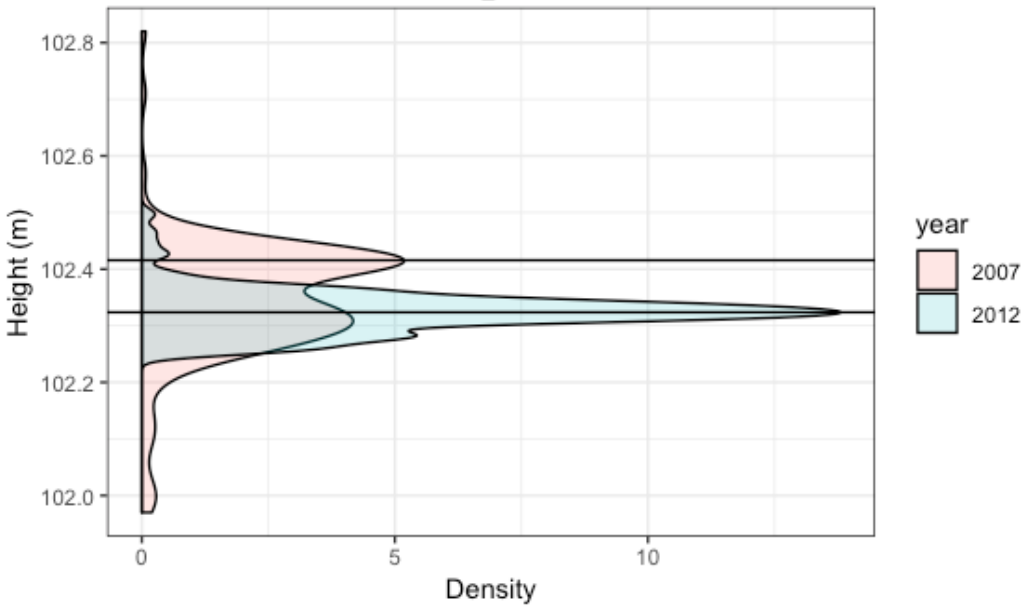
102.8
102.6
102.4
102.2
102.0
Height (m)
0
5
10
Density
year
2007
2012

7

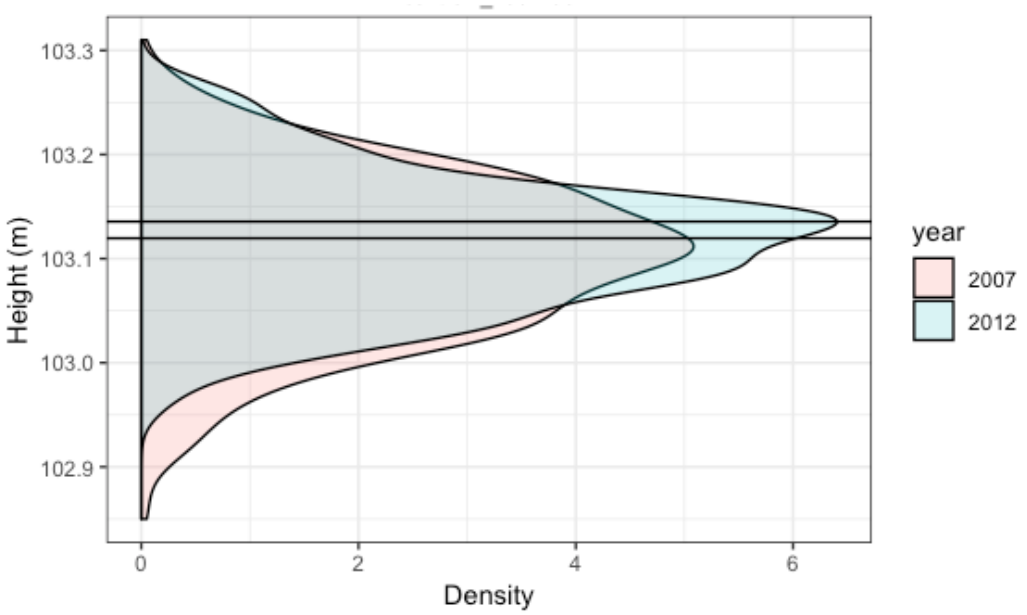
103.3
103.2
103.1
103.0
102.9
Height (m)
0
2
4
6
Density
year
2007
2012

8

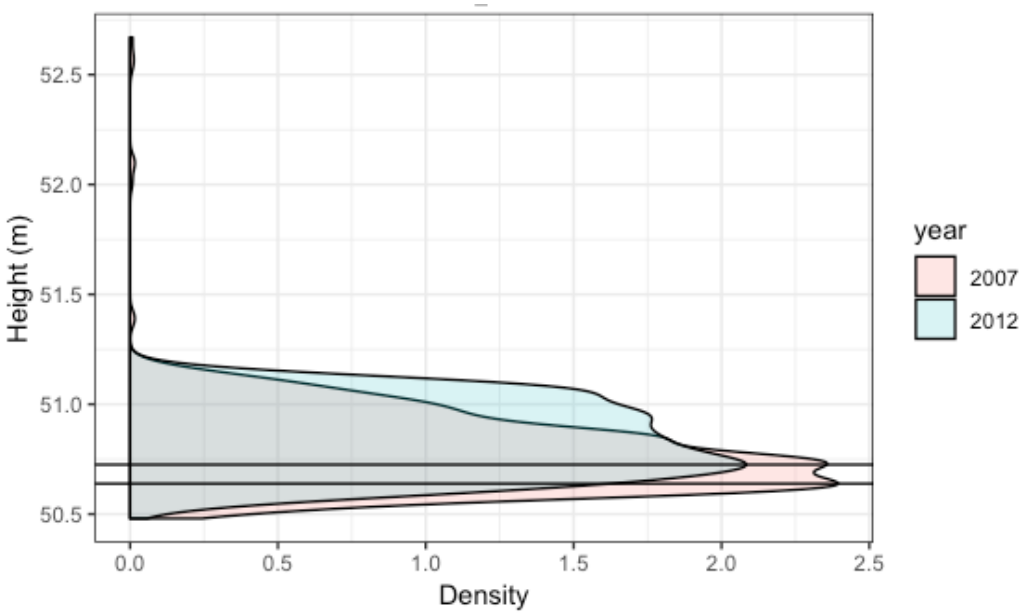
52.5
52.0
51.5
51.0
50.5
Height (m)
0.0
0.5
1.0
1.5
2.0
2.5
Density
year
2007
2012

9 N/A

10

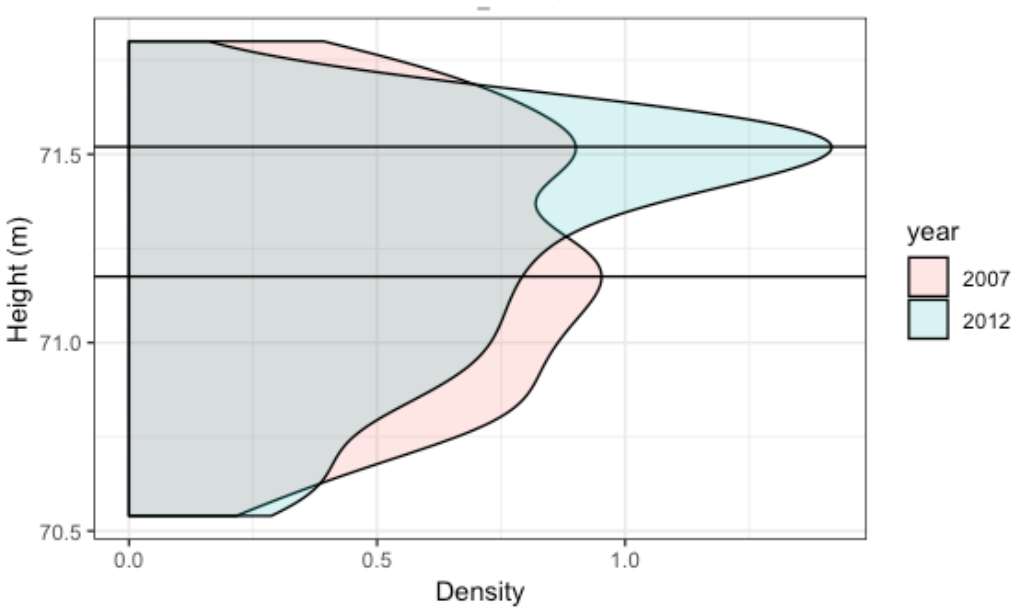
Height (m)
71.5
71.0
70.5
0.0
0.5
1.0
Density
year
2007
2012

11

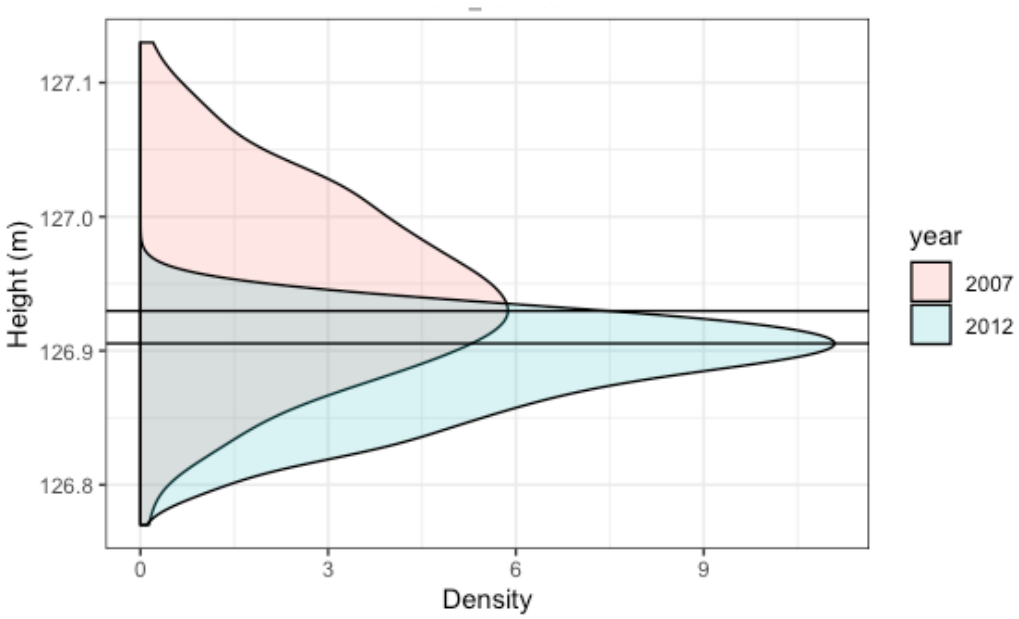
Height (m)
127.1
127.0
126.9
126.8
0
3
6
9
Density
year
2007
2012

12

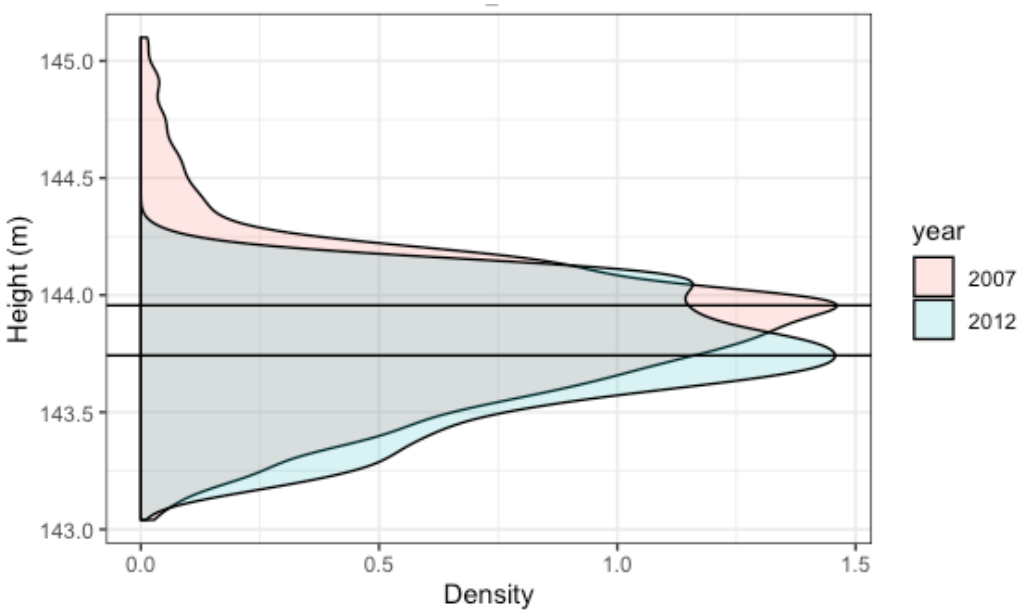
145.0
144.5
144.0
143.5
143.0
Height (m)
0.0
0.5
1.0
1.5
Density
year
2007
2012

13

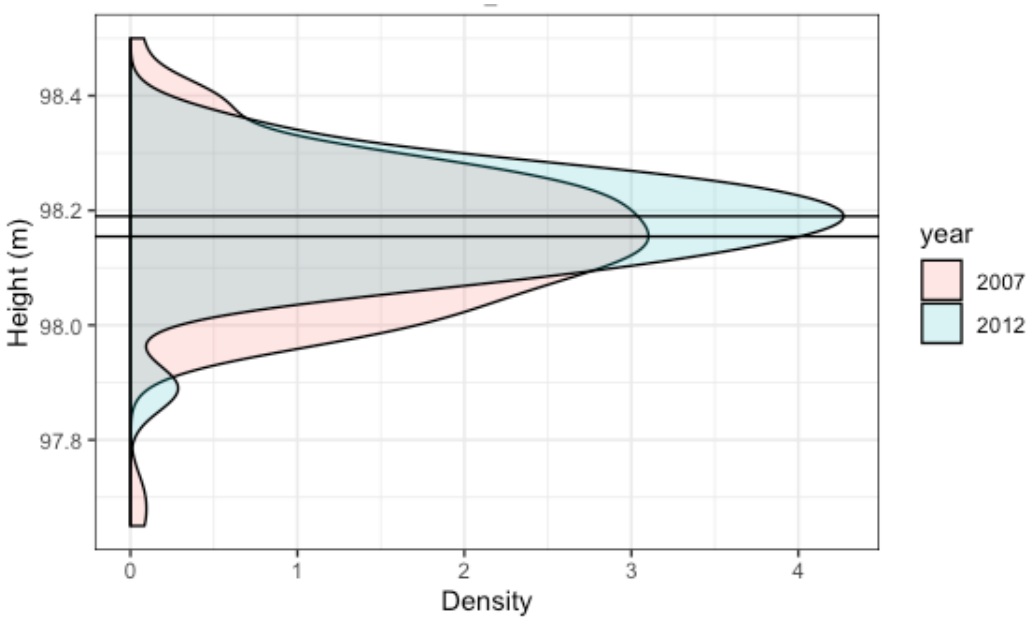
98.4
98.2
98.0
97.8
Height (m)
0
1
2
3
4
Density
year
2007
2012

14

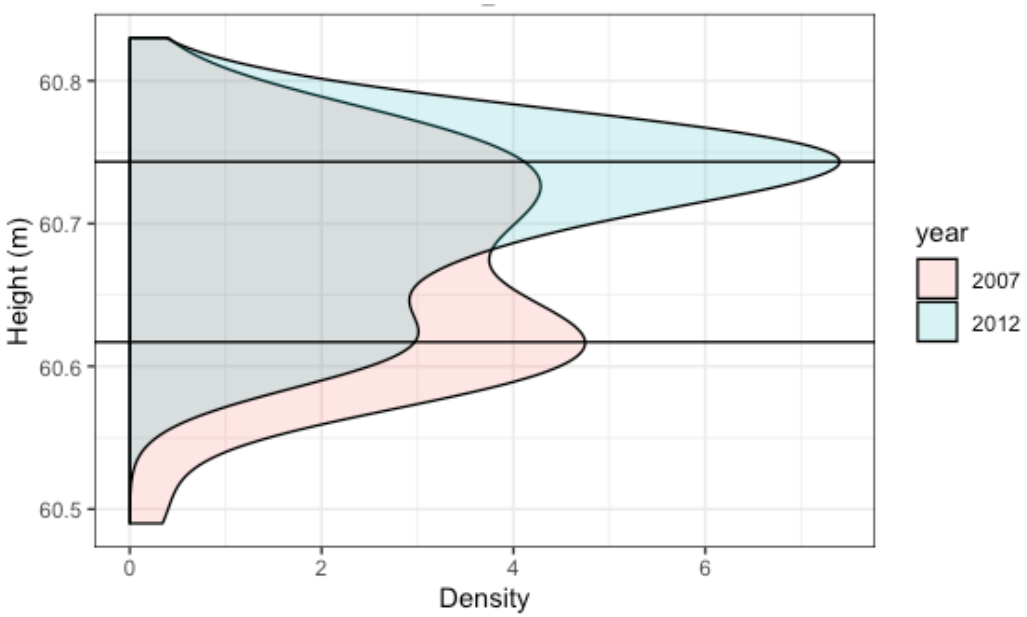
60.8
60.7
60.6
60.5
Height (m)
0
2
4
6
Density
year
2007
2012

15

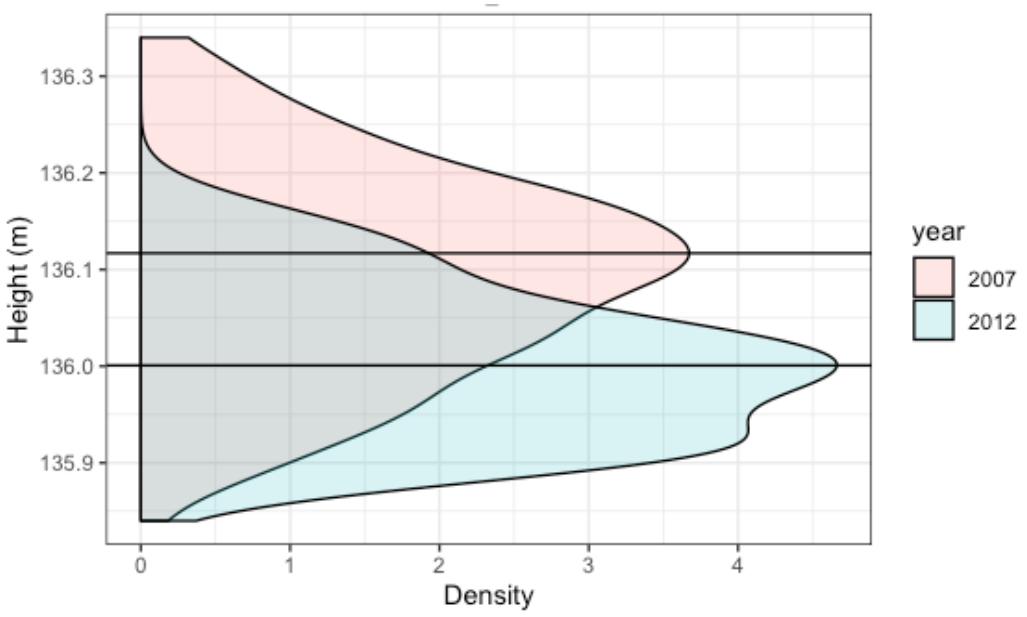
136.3
136.2
136.1
136.0
135.9
Height (m)
0
1
2
3
4
Density
year
2007
2012

16

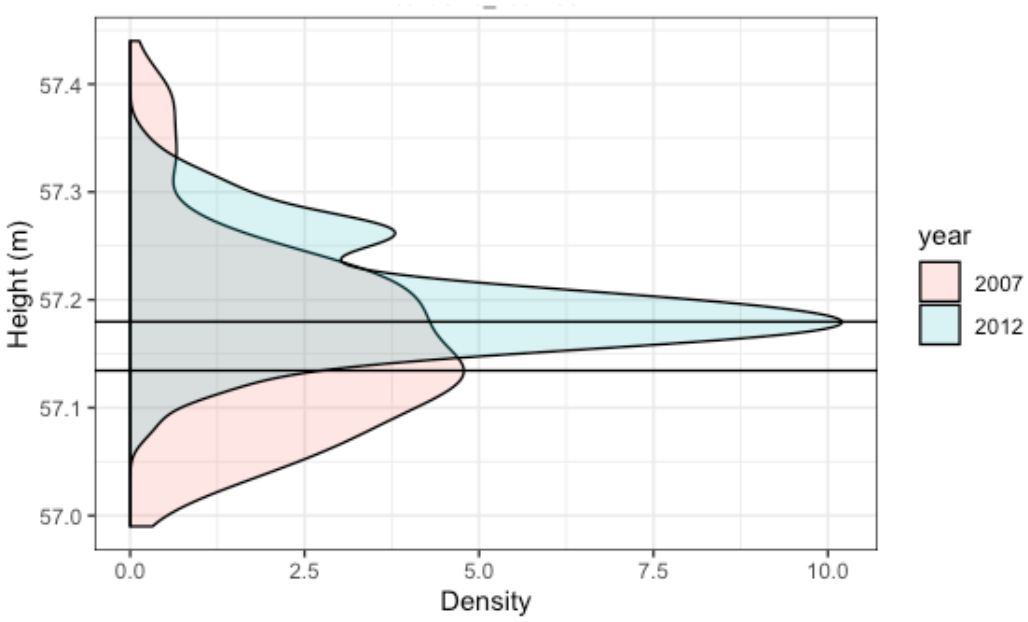
57.4
57.3
57.2
57.1
57.0
Height (m)
0.0
2.5
5.0
7.5
10.0
Density
year
2007
2012

17

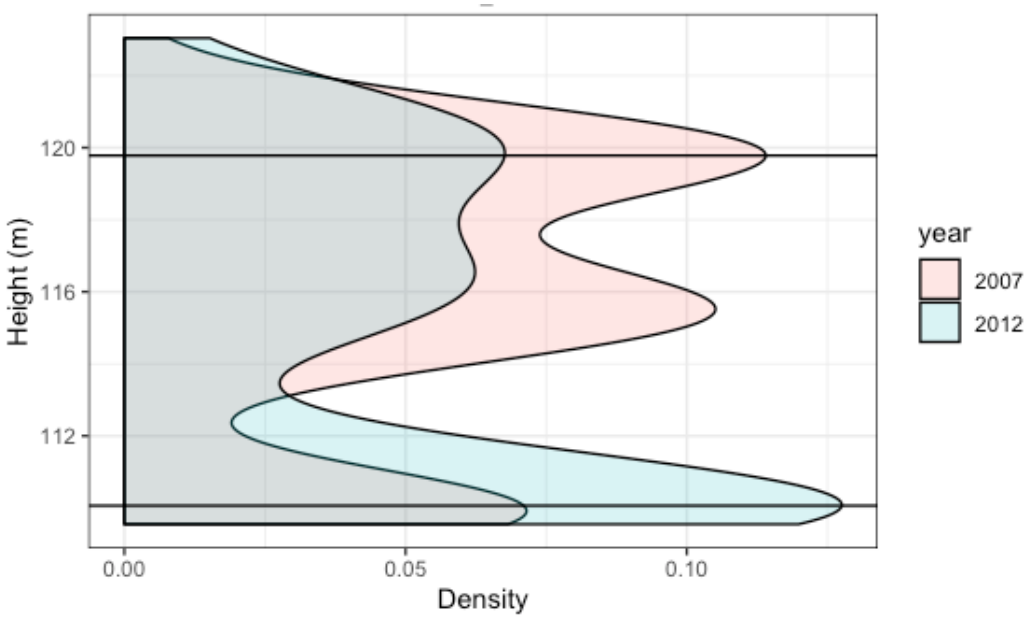
120
116
112
Height (m)
0.00
0.05
0.10
Density
year
2007
2012

18

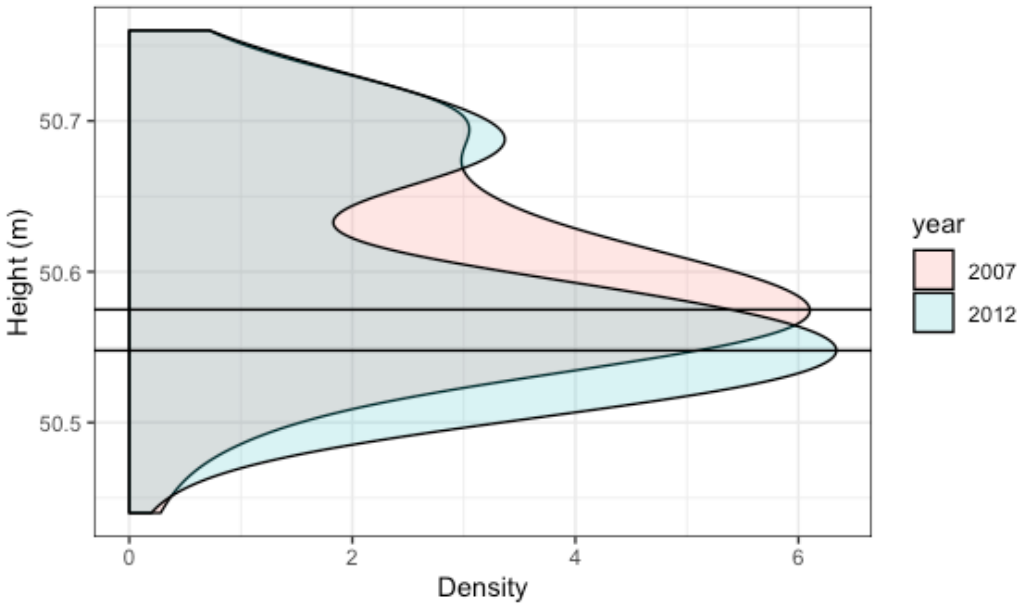
Height (m)
50.7
50.6
50.5
0
2
4
6
Density
year
2007
2012

19

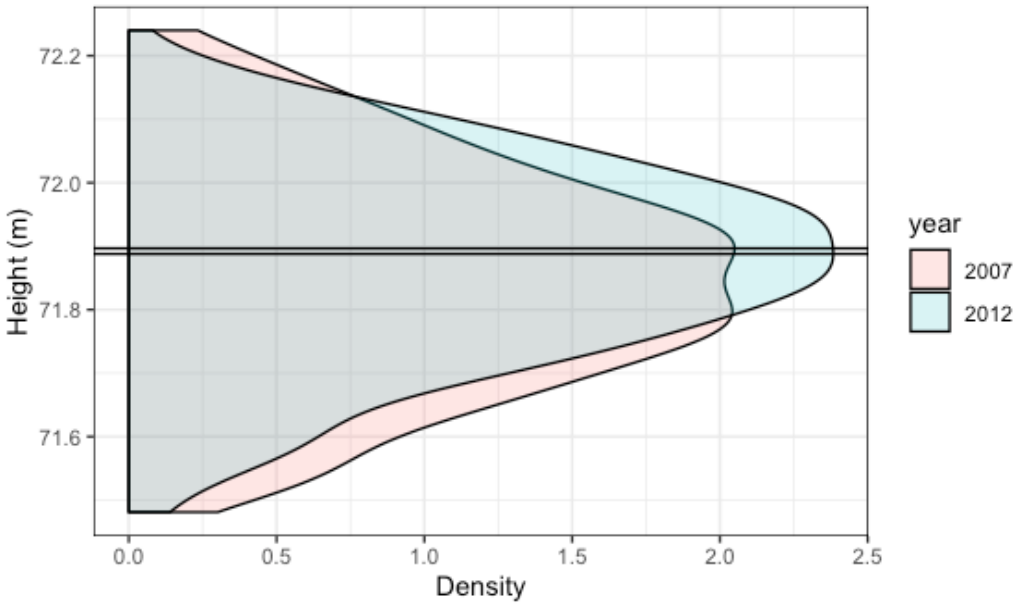
Height (m)
72.2
72.0
71.8
71.6
0.0
0.5
1.0
1.5
2.0
2.5
Density
year
2007
2012

20

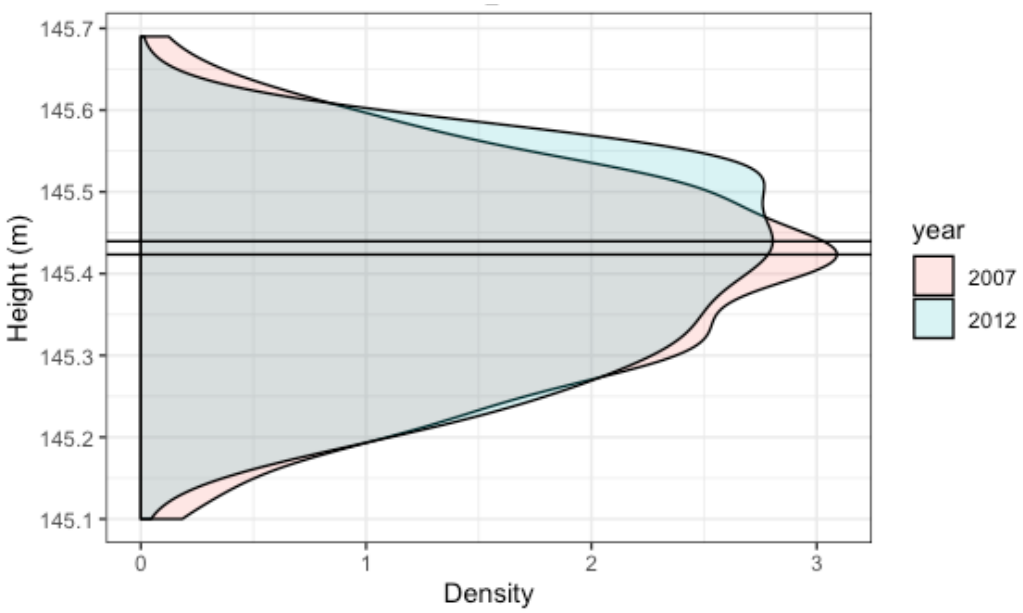
145.7
145.6
145.5
145.4
145.3
145.2
145.1
Height (m)
0
1
2
3
Density
year
2007
2012

21

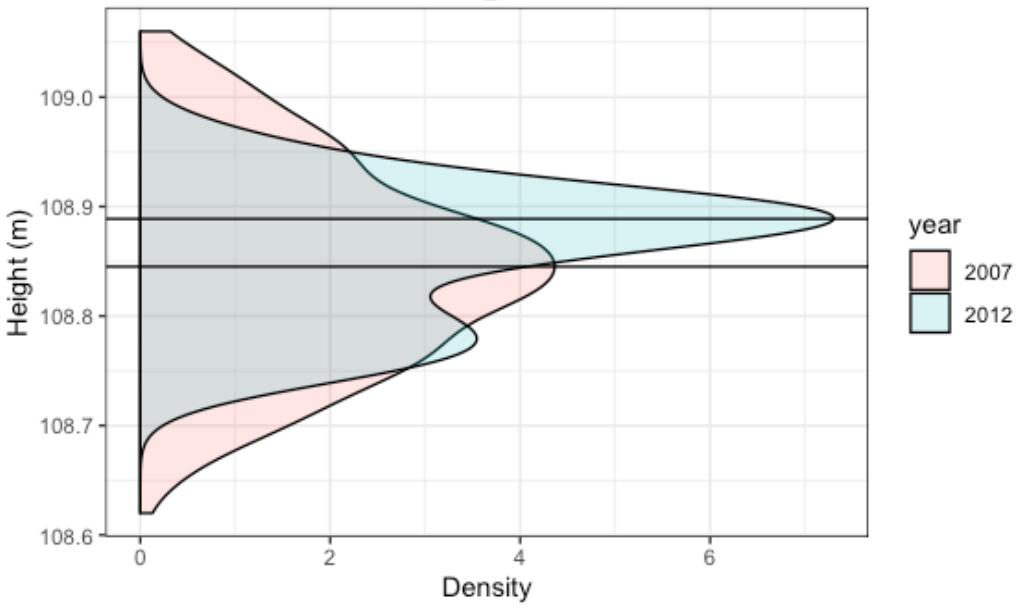
109.0
108.9
108.8
108.7
108.6
Height (m)
0
2
4
6
Density
year
2007
2012

22

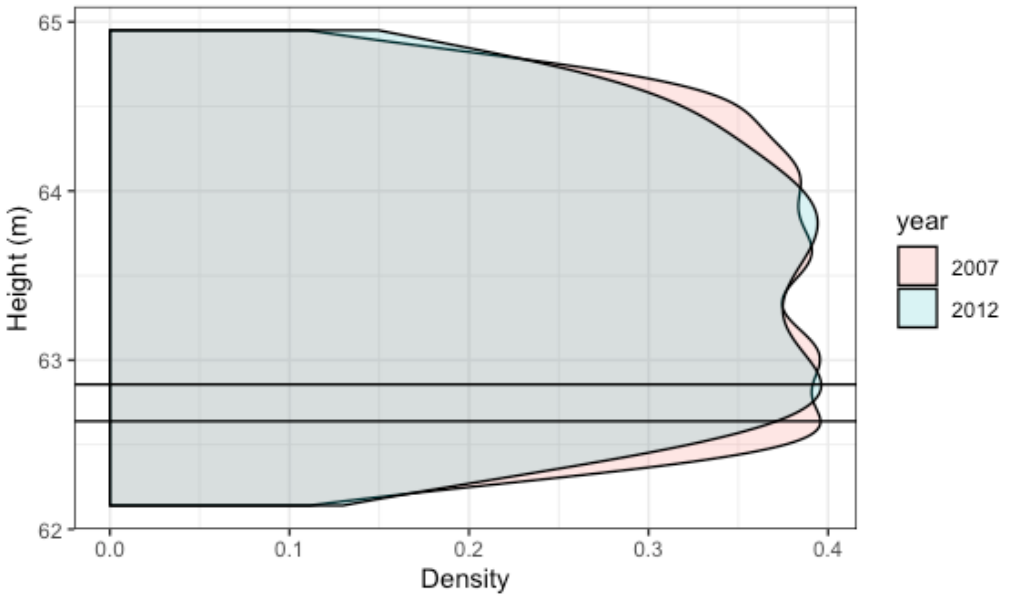

23

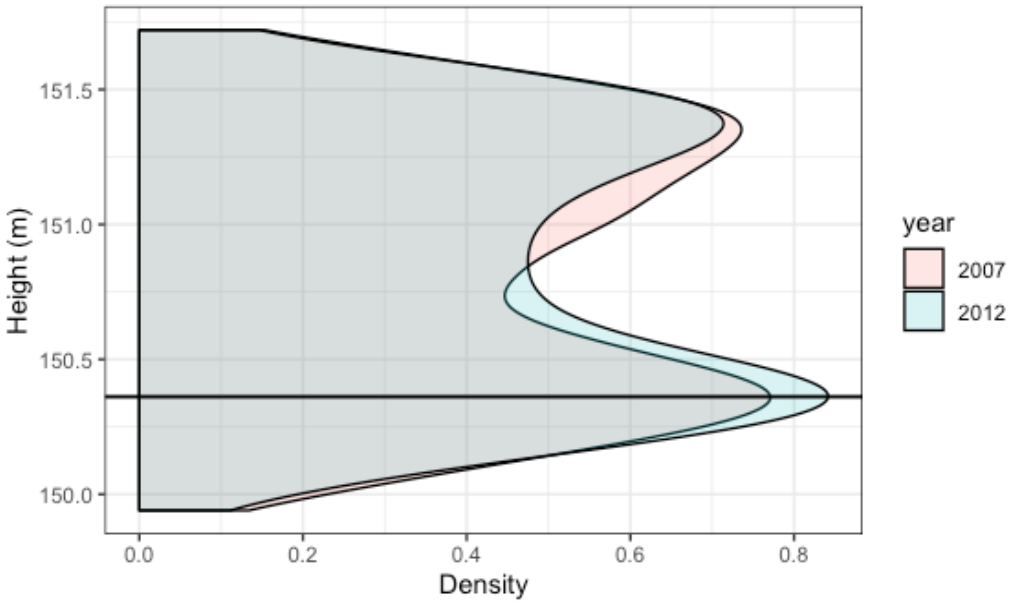

Appendix II

R script for spatial autocorrelation of control points using Moran's I.

```
# Soren Denlinger
# May 15, 2020
# Environmental Studies Honors Thesis
# spatial autocorrelation of control points

# attach necessary packages
library(spdep)
```

```
# assemble the control points and coordinates, UTM zone 19
sites <- c(2,4,6,7,8,11,13,14,15,16,17,18,19,20,21,23)
# only flat sites included
xcoord <- c(453888, 455999, 457200, 452470, 454940, 462778, 455132, 454711,
            456416, 455579, 457108, 454915, 454505, 462554, 460473, 465055)
ycoord <- c(4906444,4906081,4906679,4903420,4901650,4915037,4909024,4909332,
            4909168,4906041,4906539,4904241,4902540,4912880,4909084,4919042)
# these are the differences (2012-2007) in Z value
difference <- c(4.9, 13.3, -9.2, 1.6, 8.6, -2.4, 3.5, 12.6, -11.6, 4.5, -9.7,
                -2.7, 0.8, 1.6, 4.4, 0.4)
controls <- cbind(xcoord,ycoord)
coords <- as.matrix(controls)
controls2 <- data.frame(cbind(sites,xcoord,ycoord,difference))

# moran's I by distance, 5km search radius
control.dist  <-  dnearneigh(coords, 0, 5000) # search for neighbors
lw <- nb2listw(control.dist, style="W",zero.policy=T)  # add spatial weights
MC<- moran.mc(controls2$difference, lw, nsim=999, alternative="greater") #
results!
```

Appendix III

R script for classification, normalization, and output of lidar point clouds at two time steps.

```
# Soren Denlinger
# April 22, 2020
# Environmental Studies Honors Thesis
# processing lidar point clouds

#### ---- USER INPUT ---- ####
# enter the filepath to the folder:
filepath <- "/Volumes/Courses/ES483/ENVS_ES483_STU/soren_data/run"

# clip to shapefile?
shpBool <- F

#### ---- SET UP ---- ####
# attach necessary packages
library(lidR)
library(rgdal)
library(tidyverse)
library(ggplot2)
library(ggpmisc)

# set the working directory
setwd(filepath)
```

```
#### ---- ASSEMBLE THE FILES ---- ####

# determine number of LAS files and read them in
lasFiles <- list.files(pattern = "\\.las$")
if (shpBool == TRUE){
  shapefile <- tools::file_path_sans_ext(list.files(pattern = "\\.shp$")[1])
}
t1 <- readLAS(lasFiles[1])
t2 <- readLAS(lasFiles[2])

# set the projections to UTM zone 19
crs <- sp::CRS("+init=epsg:26919")
projection(t1) <- crs
projection(t2) <- crs
sp::identicalCRS(t1,t2)
rm(crs)

#### ---- COMPUTE THE CANOPY HEIGHT MODEL ---- ####

# clip the files
# read in the shapefile with which to clip the data
if (shpBool == TRUE){
  parcel <- readOGR(filepath, shapefile)
  t1 <- lasclip(t1, parcel)
  t2 <- lasclip(t2, parcel)
}

# classify the ground points
t1 <- lasground(t1, csf())
t2 <- lasground(t2, csf())

# normalize the las file
t1 <- lasnormalize(t1, knnidw())
t2 <- lasnormalize(t2, knnidw())

# remove the ground points to normalize any seasonal difference
t1 <- lasfilter(t1, Classification == 1)
t2 <- lasfilter(t2, Classification == 1)

# knock down the point density from the 2007 set to match 2012
t1 <- lasfilterdecimate(t1, random(0.5))

# compute the canopy height! simple as this
chm1 = grid_canopy(t1, 2, p2r(0.5))
chm2 = grid_canopy(t2, 2, p2r(0.5))
writeRaster(chm07, "chm1", format="GTiff", overwrite=TRUE)
writeRaster(chm12, "chm2", format="GTiff", overwrite=TRUE)
```

```
# generate a histogram from each chm
ggplot() + geom_histogram(aes(chm1@data@values), fill="red", alpha=0.3,
bins=50) +
  geom_histogram(aes(chm2@data@values), fill="blue", alpha=0.3, bins=50)
rm(chm1,chm2)

#### ---- CREATE VERTICAL PROFILES ---- ####

# from LAS file directly, extract x,y,z for the 2007 dataset
dat1 <- data.frame(plot_id = NA, z = NA, x = NA, y = NA)
z <- data.frame(z = t1@data$Z)
x <- data.frame(x = t1@data$X)
y <- data.frame(y = t1@data$Y)
plot_id <- data.frame(plot_id = lasFiles[1])
dat1 <- rbind(dat1, cbind(plot_id, z, x, y))
dat1 <- dat1[-1,]
dat1$year <- '2007'

# now for the 2012 dataset
dat2 <- data.frame(plot_id = NA, z = NA, x = NA, y = NA)
z <- data.frame(z = t2@data$Z)
x <- data.frame(x = t2@data$X)
y <- data.frame(y = t2@data$Y)
plot_id <- data.frame(plot_id = lasFiles[1])
dat2 <- rbind(dat2, cbind(plot_id, z, x, y))
dat2 <- dat2[-1,]
dat2$year <- '2012'

# merge the datasets, remove extraneous objects, and subset the data if need
be
totalDat <- rbind(dat1, dat2)
rm(z,x, y, plot_id)
totalDat <- subset(totalDat, z < 10 )
dat1 <- subset(dat1, z > 0 )
dat2 <- subset(dat2, z > 0 )

#### ---- VERTICAL DENSITY PLOT ---- ####
# this section is primarily for the comparison of control points

# calculate peaks
x2007int <- density(dat1$z)$x[which.max(density(dat1$z)$y)]
x2012int <- density(dat2$z)$x[which.max(density(dat2$z)$y)]
dif <- x2012int-x2007int

# plot these density peaks
ggplot(totalDat, aes(x = z, fill=year)) +
  geom_density(alpha=0.2) +
```

```
  scale_y_continuous("Density / Number of Returns") +
  scale_x_continuous("Height (m)") +
  facet_wrap(~plot_id, ncol = 3, nrow = 1) + theme_bw() +
  geom_vline(xintercept = x2007int, col="red") +
  geom_vline(xintercept = x2012int, col="blue") +
  theme(strip.background = element_blank(),
        panel.border = element_rect(colour = "black"))+
  coord_flip()

#### ---- OTHER METRICS ---- ####

# calculating some grid metrics at the voxel level
v1 = voxel_metrics(t1, .stdmetrics, 3)
v2 = voxel_metrics(t2, .stdmetrics, 3)
rm(v1,v2)

# and the grid level
m1 = grid_metrics(t1, .stdmetrics, 3)
m2 = grid_metrics(t2, .stdmetrics, 3)
md <- m2-m1
writeRaster(md, "diff_metrics", format="GTiff", overwrite=T)
writeRaster(m1, "zq2007", format="GTiff", overwrite=T)
writeRaster(m2, "zq2012", format="GTiff", overwrite=T)
rm(m1,m2,md)

# function to remove outliers - courtesy of Jean-Romaine Roussel
lasfilternoise = function(las, ...){
  UseMethod("lasfilternoise", las)
}

lasfilternoise.LAS = function(las, sensitivity){
  p95 <- grid_metrics(las, ~quantile(Z, probs = 0.95), 10)
  las <- lasmergespatial(las, p95, "p95")
  las <- lasfilter(las, Z < p95*sensitivity)
  las$p95 <- NULL
  return(las)
}
# execute the function if the dataset is especially noisy
t1 <- lasfilternoise(t1, sensitivity = 1.2)
t2 <- lasfilternoise(t2, sensitivity = 1.2)
```

Appendix IV

R script for analysis of height difference rasters.

```
# Soren Denlinger
# May 15, 2020
# Environmental Studies Honors Thesis
```

```
# statistical analysis of difference rasters

# attach any necessary packages
library(raster)
library(rgdal)
library(ggplot2)
library(dplyr)
library(MASS)

#### ---- growth differences for forest types (box plots) ---- ####
# read in growth rasters for each forest height -> change x to name of each
ripGrowth <- raster(x = "rzq95dif_export.tif")
wetGrowth <- raster(x = "wz95dif_export.tif")
upGrowth <- raster(x = "uzq95dif_export.tif")

# manipulate their extents by determining the extremes of each
xmin <- max(bbox(ripGrowth)[1,1], bbox(wetGrowth)[1,1], bbox(upGrowth)[1,1])
xmax <- min(bbox(ripGrowth)[1,2], bbox(wetGrowth)[1,2], bbox(upGrowth)[1,2])
ymin <- max(bbox(ripGrowth)[2,1], bbox(wetGrowth)[2,1], bbox(upGrowth)[2,1])
ymax <- min(bbox(ripGrowth)[2,2], bbox(wetGrowth)[2,2], bbox(upGrowth)[2,2])
newextent=c(xmin, xmax, ymin, ymax)
# then set the extent of each raster to that maximum to preserve data
ripGrowth = crop(ripGrowth, newextent)
wetGrowth = crop(wetGrowth, newextent)
upGrowth = crop(upGrowth, newextent)
rm(xmax, xmin, ymax, ymin, newextent)

# put the rasters in a rasterbrick for easy plotting
growthStack <- stack(ripGrowth, wetGrowth, upGrowth)
growthBrick <- brick(growthStack)
growthDif <- as.data.frame(growthBrick, xy=F)
rm(growthBrick, growthStack, ripGrowth, upGrowth, wetGrowth)

# clean the data in each layer
# produce one dataset for all data, positive and negative
growthDif1 <- growthDif %>%
  rename(UplandGrowth = uzq95dif_export,
         WetlandGrowth = wz95dif_export,
         RiparianGrowth = rzq95dif_export) %>%
  mutate(UplandGrowth = UplandGrowth*100,
         WetlandGrowth = WetlandGrowth*100,
         RiparianGrowth = RiparianGrowth*100)
# produce a second for only positive data
growthDif2 <- growthDif %>%
  rename(UplandGrowth = uzq95dif_export,
         WetlandGrowth = wz95dif_export,
         RiparianGrowth = rzq95dif_export) %>%
  mutate(UplandGrowth = UplandGrowth*100,
```

```
         WetlandGrowth = WetlandGrowth*100,
         RiparianGrowth = RiparianGrowth*100)
growthDif2$UplandGrowth <- replace(growthDif2$UplandGrowth,
which(growthDif2$UplandGrowth < 0), NA)
growthDif2$WetlandGrowth <- replace(growthDif2$WetlandGrowth,
which(growthDif2$WetlandGrowth < 0), NA)
growthDif2$RiparianGrowth <- replace(growthDif2$RiparianGrowth,
which(growthDif2$RiparianGrowth < 0), NA)

# stack the data for an ANOVA
growthDif2_stack <- stack(growthDif2)
gd2_anova <- aov( values ~ ind, growthDif2_stack)
gd2_tukey <- TukeyHSD(gd2_anova) # results HERE

# calculate specific means and medians for ALL changes
ripVals <- na.omit(growthDif1$RiparianGrowth)
ripMean <- mean(ripVals)
ripMed <- median(ripVals)
wetVals <- na.omit(growthDif1$WetlandGrowth)
wetMean <- mean(wetVals)
wetMed <- median(wetVals)
upVals <- na.omit(growthDif1$UplandGrowth)
upMean <- mean(upVals)
upMed <- median(upVals)
rm(ripVals, ripMean, ripMed, wetVals, wetMean, wetMed, upVals, upMean, upMed)

# calculate specific means and medians for GROWTH
posripVals <- na.omit(growthDif2$RiparianGrowth)
posripMean <- mean(posripVals)
posripMed <- median(posripVals)
poswetVals <- na.omit(growthDif2$WetlandGrowth)
poswetMean <- mean(poswetVals)
poswetMed <- mean(poswetVals)
posupVals <- na.omit(growthDif2$UplandGrowth)
posupMean <- mean(posupVals)
posupMed <- median(posupVals)
rm(posripMean, posripVals, posripMed, poswetMean, poswetVals, posupMean,
posupVals)

# plot the box plots for all data, both positive and negative
p1 <- ggplot(stack(growthDif1), aes(x = ind, y = values)) +
geom_hline(yintercept=0) +
  geom_boxplot(outlier.shape = NA, fill="lightgreen") +
  coord_cartesian(ylim = c(-400, 450)) + ylab("Change in Centimeters") +
xlab("Forest Type") +
  theme(axis.text = element_text(size=10, family='serif'),
        axis.title = element_text(size=12, family="serif"))
# save the plot
```

```
ggsave("all95thboxplot.png", plot=p1, width=5, height=3, units="in",
device="png")

# plot the box plots for only positive data
p2 <- ggplot(stack(growthDif2), aes(x = ind, y = values)) +
geom_hline(yintercept=0) +
  geom_boxplot(outlier.shape = NA, fill="lightgreen") +
  coord_cartesian(ylim = c(-25, 450)) + ylab("Change in Centimeters") +
xlab("Forest Type") +
  theme(axis.text = element_text(size=10, family='serif'),
        axis.title = element_text(size=12, family="serif"))
# save the plot
ggsave("pos95thboxplot.png", plot=p2, width=5, height=3, units="in",
device="png")

# remove the above datasets to save memory
rm(gd2_anova, gd2_tukey, growthDif, growthDif2, growthDif1, growthDif2_stack)

#### ---- forest growth by height (scatter plots) ---- ####
# read in the rasters
# riparian data
r1 <- raster(x = "rip2007_z95.tif") # load in 2007 heights
r1[r1 < 0.1] <- NA # set any values below 0.1 to NA to exclude non-trees
r2 <- raster(x = "rz95difpos.tif") # load in difference raster (growth)

# repeat for wetlands data
w1 <- raster(x = "wet2007_z95.tif")
w1[w1 < 0.1] <- NA
w2 <- raster(x = "w2_extent.tif") # this file doesn't fit the rest of the
                                  # pattern due to necessary modifications
                                  # to its extent in ArcGIS

# repeat for upland data
u1 <- raster(x = "up2007_z95.tif")
u1[u1 < 0.1] <- NA
u2 <- raster(x = "uzq95difpos.tif")

# manipulate their extents, similar to above
xmin <- max(bbox(r1)[1,1], bbox(u1)[1,1], bbox(w1)[1,1], bbox(w2)[1,1])
xmax <- min(bbox(r1)[1,2], bbox(u1)[1,2], bbox(w1)[1,2], bbox(w2)[1,2])
ymin <- max(bbox(r1)[2,1], bbox(u1)[2,1], bbox(w1)[2,1], bbox(w2)[2,1])
ymax <- min(bbox(r1)[2,2], bbox(u1)[2,2], bbox(w1)[2,2], bbox(w2)[2,2])
newextent=c(xmin, xmax, ymin, ymax)
# crop each raster to fit this new extent, making them identical
r1 = crop(r1, newextent)
r2 = crop(r2, newextent)
u1 = crop(u1, newextent)
u2 = crop(u2, newextent)
```

```
w1 = crop(w1, newextent)
w2 = crop(w2, newextent)
rm(xmax, xmin, ymax, ymin, newextent)

# convert the rasters to a stack, then brick, then dataframe
ripHeights <- as.data.frame(brick(stack(r1, r2)) , xy=F)
# filter out NA values
ripHeights <- filter(ripHeights, !is.na(rip2007_z95), !is.na(rz95difpos))
# remove starting heights below 2 (represent a separate batch of noise)
ripHeights <- filter(ripHeights, rip2007_z95>2)
# run bisquare regression on the data to find slope
rip.r <- MASS::rlm( rz95difpos ~ rip2007_z95, dat=ripHeights,
psi="psi.bisquare")
# plot riparian data
h1 <- ggplot(ripHeights, aes(rip2007_z95, rz95difpos)) +
  geom_point(color="green4", alpha=0.1) +
  geom_smooth(method=MASS::rlm, color="black", method.args=
list(psi="psi.bisquare")) +
  xlab("Height in 2007 (m)") + ylab("Growth in 2012 (m)") +
  ggtitle("Riparian Forest Growth by 2007 Height") +
  theme(axis.title = element_text(size=12, family="serif"),
        plot.title = element_text(size=12, family="serif"))
# save the plot
ggsave("ripHeightsScatter.png", plot=h1, width=6, height=3.5, units="in",
device="png")

# convert the rasters to a stack, then brick, then dataframe
upHeights <- as.data.frame(brick(stack(u1, u2)) , xy=F)
# filter out NA values
upHeights <- filter(upHeights, !is.na(up2007_z95), !is.na(uzq95difpos))
# remove starting heights below 2 (represent a separate batch of noise)
upHeights <- filter(upHeights, up2007_z95>2)
# run bisquare regression on the data to find slope
up.r <- MASS::rlm( uzq95difpos ~ up2007_z95, dat=upHeights,
psi="psi.bisquare")
# plot uplands data
h2 <- ggplot(upHeights, aes(up2007_z95, uzq95difpos)) +
  geom_point(color="green4", alpha=0.1) +
  geom_smooth(method=MASS::rlm, color="black",method.args=
list(psi="psi.bisquare")) +
  xlab("Height in 2007 (m)") + ylab("Growth in 2012 (m)") +
  ggtitle("Upland Forest Growth by 2007 Height") +
  theme(axis.title = element_text(size=12, family="serif"),
        plot.title = element_text(size=12, family="serif"))
# save the plot
ggsave("upHeightsScatter.png", plot=h2, width=6, height=3.5, units="in",
device="png")
```

```
# convert the rasters to a stack, then brick, then dataframe
wetHeights <- as.data.frame(brick(stack(w1, w2)) , xy=F)
# filter out NA values
wetHeights <- filter(wetHeights, !is.na(wet2007_z95), !is.na(w2_extent))
# remove starting heights below 2 (represent a separate batch of noise)
wetHeights <- filter(wetHeights, wet2007_z95>2)
# run bisquare regression on the data to find slope
wet.r <- MASS::rlm( w2_extent ~ wet2007_z95, dat=wetHeights,
psi="psi.bisquare")
# plot wetlands data
h3 <- ggplot(wetHeights, aes(wet2007_z95, w2_extent)) +
  geom_point(color="green4", alpha=0.1) +
  geom_smooth(method=MASS::rlm, color="black", method.args=
list(psi="psi.bisquare")) +
  xlab("Height in 2007 (m)") + ylab("Growth in 2012 (m)") +
  ggtitle("Wetland Forest Growth by 2007 Height") +
  theme(axis.title = element_text(size=12, family="serif"),
        plot.title = element_text(size=12, family="serif"))
# save the plot
ggsave("wetHeightsScatter.png", plot=h3, width=6, height=3.5, units="in",
device="png")
```